Ph.D. DISSERTATION

LIQUID-CAPPED ENCODED MICROCAPSULE FOR MULTIPLEX ASSAYS

다중 분석을 위한 코드화된 마이크로캡슐 제작

BY

YOUNGHOON SONG

AUGUST 2017

DEPARTMENT OF ELECTRICAL ENGINEERING AND
COMPUTER SCIENCE
COLLEGE OF ENGINEERING
SEOUL NATIONAL UNIVERSITY

Ph.D. DISSERTATION

LIQUID-CAPPED ENCODED MICROCAPSULE FOR MULTIPLEX ASSAYS

다중 분석을 위한 코드화된 마이크로캡슐 제작

YOUNGHOON SONG

AUGUST 2017

DEPARTMENT OF ELECTRICAL ENGINEERING AND
COMPUTER SCIENCE
COLLEGE OF ENGINEERING
SEOUL NATIONAL UNIVERSITY

LIQUID-CAPPED ENCODED MICROCAPSULE FOR MULTIPLEX ASSAYS

다중 분석을 위한 코드화된 마이크로캡슐 제작

지도교수 권 성 훈

이 논문을 공학박사 학위논문으로 제출함

2017 년 8 월

서울대학교 대학원

전기컴퓨터 공학부

송 영 훈

송영훈의 공학박사 학위논문을 인준함

2017 년 8 월

위 원 장 : _____박 영 준_____(인)

부위원장 : _____권 성 훈_____(인)

위 원 : _____김 성 재_____(인)

위 원 : _____서 종 모_____(인)

위 원 : _____박 욱_____(인)

Abstract

LIQUID-CAPPED ENCODED MICROCAPSULE FOR MULTIPLEX ASSAYS

YOUNGHOON SONG

DEPARTMENT OF ELECTRICAL ENGINEERING AND COMPUTERSCIENCE

COLLEGE OF ENGINEERING

SEOUL NATIONAL UNIVERSITY

In this dissertation, I introduce a new platform for the multiplex assays that enables the handling of thousands of different liquids in nanoliter volume. Handling tiny volume of liquids requires compartmentalization of precise volumes of the liquid, while preventing evaporation of the liquid in the air. Currently, the most representative method for handling small volume of the liquids is the droplet microfluidics, which compartmentalizes liquid droplets in immiscible oil phase to prevent the evaporation of the nanoliter volume of the liquid. The droplet microfluidics has been studied for more than a decade and the technology has now been applied in various biochemical

applications such as drug screening, PCR enrichment for targeted sequencing and rare cell detection. Although its impact is already obvious in some applications, at present, the droplet microfluidics is used to analyze hundreds of thousands of aliquots of a single type of an analyte solution and there are few methods to process different analytes. Unlike common macroscale liquid carriers such as tubes and wells, which can be easily labeled to know their contents, the droplets are difficult to be labeled. To allow the droplet microfluidics with many different types of analytes, it would be necessary to label the droplets with a number of identification codes. In this dissertation, I solved this problem of labeling through the development of the 'encoded microcapsules'.

First, I developed the microfluidic device that enables to encapsulate nanoliter liquid inside the solid Teflon microcapsule. Teflon is chemically and biologically inert and highly flexible. These properties of the Teflon enable to encapsulate the liquid stably without evaporation and cross-contamination. I found that a photoinitiator mixed with the Teflon has photoluminescence property after the exposure to the UV light. Using this property, for the first time, I engraved graphical codes on the shell of the microcapsule to label the liquid held inside. This graphical code enables to handle numerous kinds of liquids and to make a pooled chemical library by mixing and storing the differently encoded microcapsules in a tube.

For the multiplex assay with the encoded microcapsule, I also developed a

microwell array platform that enables to assemble thousands of heterogeneous encoded microcapsules in the microwell array by a single pipetting process. The graphical codes on the microcapsules can be used to identify each liquid in the microcapsule even when they are randomly positioned in the microwells. To release the liquid inside the microcapsule, I also developed a laser releasing system for selective releasing and a mechanical releasing system for high-throughput releasing.

To validate that the platform can be used for various liquid-liquid or liquid-cell reactions, I performed an enzyme inhibitor screening with the β-galactosidase, a virus transduction, and a drug-induced apoptosis test using osteosarcoma cells (U2OS) and anticancer drugs. The results including the dose-response curves and the corresponding IC50 values of the enzyme inhibitor screening and cell viabilities of the drug-induced apoptosis test showed good agreement with the results obtained using a conventional well-plate platform, confirming that the encoded microcapsule can be an efficient alternative liquid-format screening platform.

Keywords: Encoded microcapsule, Liquid encapsulation, Droplet labeling, Multiplex assay

Student Number: 2009-23116

Contents

List of Figures

List of Tables

Chapter 1

Introduction

In this dissertation, I introduce a new platform for multiplex assays that enables to handle thousands of different liquids in nanoliter volume. Handling tiny volume of the liquids requires the compartmentalization of precise volume of liquid while preventing evaporation of liquid in air. The key ideas are the development of the encoded microcapsule that can encapsulate liquid inside and the self-assembly of these encoded microcapsules in the microwell array. In addition, by developing the liquid releasing platform, I also demonstrate that these encoded microcapsules can be applied to various liquid-liquid or liquid-cell based assays.

In chapter 1, I introduce a droplet microfluidics as a small volume liquid handling technology and describe the advantage and the applications of the droplet microfluidics. And, for multiplex assay applications with the droplet microfluidics, I

describe a few droplet labelling technologies categorized to spectral encoding and positional encoding. Lastly, the main concept of my work is described, which combines the droplet microfluidics with the lithographical technology.

In chapter 2, I introduce the generation of the liquid-capped microcapsule using the microfluidic device. The double emulsion droplet was generated by flow rate control of the microfluidic device, and the microcapsule was fabricated by the UV polymerization of a photo-curable Teflon phase of the double emulsion. Properties of the microcapsule were analyzed by leakage test, off-centering measurement and long-time storage test of the liquid inside the microcapsule.

In chapter 3, the encoding method of the microcapsule is described. I found that the DMPA photoinitiator mixed with the Teflon polymer displayed photoluminescence property after the exposure to the UV light. The characteristic of the DMPA after the UV exposure is first analyzed and the encoding process utilizing the patterned UV light is described. Also, the characteristics of graphical code in the microcapsule such as code diversity, variation of fluorescence intensity according to the UV light, and code durability are analyzed.

In chapter 4, a microwell array platform with the encoded microcapsule is developed for the multiplex assay applications. First, fabrication processes of the microwell and the micro pillar array are described. Then, assembly process of the encoded microcapsule is described. To estimate the code distribution of the encoded

microcapsule after the assembly, theoretical analysis with simulation of the binomial distribution is performed and compared with experimental result. Methods for releasing of the liquid inside the microcapsule are also described.

In chapter 5, to validate that our platform can be used for various liquid-liquid or liquid-cell reactions, I perform an enzyme inhibitor screening with the β-galactosidase, a virus transduction and a drug-induced apoptosis test using osteosarcoma cells (U2OS) and anticancer drugs. The results including the dose-response curves and the corresponding IC50 values of the enzyme inhibitor screening and the cell viabilities of the drug-induced apoptosis test are compared with the results obtained using a conventional well-plate platform, confirming that the encoded microcapsule can be an efficient alternative liquid-format screening platform.

1.1 Introduction of the Droplet Microfluidics

The droplet microfluidics has been studied extensively for more than a decade due to its capability of handling small volume of liquids in a highly parallel manner. Millions of the droplets formed by compartmentalization of an aqueous liquid in a immiscible oil phase works as 'tiny reaction tubes' that is intrinsically millions of aliquots of a bulk liquid. Each droplet is regarded as an individual reaction chamber, and the volume of liquid can be precisely controlled using microfluidic devices. The immiscible oil phase surrounding the droplets provides physical and chemical isolation of the droplets, preventing cross contamination and evaporation.

The droplet microfluidics has been studied widely [1] because of its merits in biochemical assays. Main advantages of the droplet microfluidics include the ability to handle small volume of liquid, increased reaction performance compared to macroscale reaction, low cost according to low sample consumption, and ability to perform a large number of individual experiments simultaneously. In addition, high surface to volume ratio and short diffusion length provide significantly decrease reaction times. The technology has now been applied in various biochemical applications such as molecular detections, drug delivery, diagnosis chip and cell biology [2-19].

Table 1.1 Recent applications of droplet microfluidics

Application	**Molecular detection**	**Drug delivery**	**Diagnosis chip**	**Cell biology**
Target / System	Bovine angiogenin dsDNA Glucose Quinones β-Galactosidase Bovine serum albumin Avid in Streptavidin	Bovine serum albumin Lipid vehicle Gelatin-alginate Ampicillin 5-fluorouracil doxorubicin hydrochloride Poly lactic-co-glycolic acid	*Staphylococcus aureus* Prostate-specific antigen Cocaine Plasma and blood cells Human angiogenin Oligomer amyloid β Influenza Circulating tumor cell Virus Protein kinase Multi-nucleotide polymorphism	Cancer cell Mouse hybridoma cell HL-60 cell HeLa cell *Escherichia coli* Yeast cell Human lymphoid cell Antibody-secreting cell

1.2 Principles of Droplet Microfluidics

The principle of the droplet generation is based on two immiscible liquids where the disperse phase for the droplet is injected into the immiscible continuous phase, surrounding the droplets. For the droplet formation in microscale, the interfacial forces and viscous forces are dominant. The relative strength of these two forces is represented by the dimensionless capillary number *Ca*, expressed by $Ca = \mu v/\sigma$. Here, μ is generally the viscosity of the most viscous fluid in two-phase system, v is the velocity of that phase, and σ is the interfacial tension between the dispersed and continuous phase.

The capillary number of the flow can be changed by changing the flow rate of the continuous phase. As the flow rate of the continuous phase is increased, the capillary number is increase and the interfacial force is dominant. In contrast, as the flow rate of the continuous phase is decreased, the capillary number is decreased and the viscous force is dominant. The interfacial tension tends to reduce the interfacial area, which is important in the formation of droplets and their stability. The viscous force act to extend and stretch the interface. At low *Ca* (<1), the interfacial tension is dominant and spherical droplets are generated. In contrast, at high *Ca* (>>1), the viscous forces are dominant, leading to deformation of the droplets [20].

The disperse phase can be chemical drug, protein, DNA or cells contained in aqueous liquid. The continuous phases include hydrocarbon and fluorocarbon oils which are not mixed with the droplet phase. Usually, the continuous phase includes a surfactant according to the material used in continuous phase. The surfactant is necessary for the droplet formation and stable maintenance of the droplets which prevent droplet coalescence. For the chemical and the biological applications, droplet should have constant properties such as size of the droplets, shape, monodispersity and resistance to coalescence.

Table 1.2 Reported components of droplet emulsions in microfluidics [21]

Type of emulsion	Continuous phase	Surfactants	Geometry
Fluorinated oils			
W/O	1*H*,1*H*,2*H*,2*H*-Perfluorodecyltrichlorosilane, Fluorinert FC 3283; FC 40	PEPE–PEG; PFPE–PEG–PFPE triblock copolymers; PFPE–PEG–gold diblock surfactants (home-made); EA surfactant	T-junction; flow-focusing
	Fluorinated HFE-7500	EA surfactant; Krytox–Jeffamine–Krytox A–B–A triblock copolymer	Flow focusing
	Fluorinert FC 40	PFPE–PEG block copolymer	Flow-focusing
	Fluorinert FC 70, FC 40	PEPE–PEG	T-junction; flow-focusing
Hydrocarbon oils			
W/O	Mineral	Span 80; Tween 80	Main channel to the flow rate in the external access channel
	Hexadecane	Span 80	Single T, K-junction
O/W	Soybean; hexadecane, silicon	PEG, sodium dodecyl sulphate (SDS)	Flow-focusing
	Mineral; silicon	Pluronic F-68	T-junction
	n-Hexadecane	SDS	T-junction
G/L	Nitrogen	Dispersed phase – deionized water (90% (v/v) glycerol; 2 wt% SDS)	Flow-focusing
L/G	Propane, butane, air	2 wt% Tween-20	T-junction

1.2.1 Geometries for droplet generation

To produce monodisperse droplets with size of microscale. The confinement factor (geometry) also has to be considered along with the capillary number [22] and the microfluidic device with special geometries are necessary. The representative geometries for generation of the droplets include T-junction, flow focusing and co-flowing microfluidic structures.

The T-junction geometry is one of the most common geometry used to generate the droplets. The vertical inlet channel contained dispersed phase and the main horizontal channel contains continuous phases. These two channels intersect typically orthogonally and the droplets are generated at the intersection of the two channels. By adding microvalve to the inlet channel, on-demand generation of the droplet is also possible.

In the flow focusing geometry, two symmetric vertical channels contain continuous phase and horizontal channel contains disperse phase. As the dispersed phase flows into the intersection, the continuous phase forces the dispersed phase through a small orifice leading into a larger channel filled with the continuous phase and the droplets are generated. In the flow focusing, droplet size, generation frequency of the droplet can be controlled through changing the flow rates of dispersed phase and continuous phase, viscosity of the phase and the size of orifice.

In the co-flow geometry, the dispersed phase is forced through a small capillary centered inside a larger diameter channel with the continuous phase following parallel to the dispersed phase. there are two types of droplet generation process. One is dripping and the other is jetting. At low flor rates, dripping is dominant because of absolute instability as the forces acting on the stream of water at a specific frequency and location in the stream. At higher flow rate, jetting is dominant because of convective instabilities Droplet formation in co-flow geometry is highly affected by

fluid velocities, viscosities, surface tension of the flow. [21].

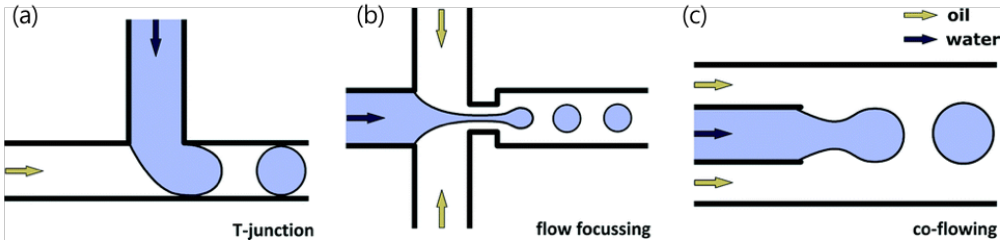

Figure 1.1 Three principle microfluidic geometries for droplet generation. (a) In T-junction, the vertical inlet channel contained dispersed phase and the main horizontal channel contains continuous phases. These two channels intersect typically orthogonally and droplets are generated at the intersection of the two channels (b) In flow focusing, two symmetric vertical channels contain continuous phase and horizontal channel contains disperse phase. As the dispersed phase flows into the intersection, the continuous phase forces the dispersed phase through a small orifice leading to generate droplets. and (c) In co-flowing, the dispersed phase is forced through a small capillary centered inside a larger diameter channel with the continuous phase following parallel to the dispersed phase [23].

1.2.2 Fundamental models of droplet generation.

There are five fundamental models of shear-based droplet generation: squeezing, dripping, jetting, tip-streaming and tip-multi-breaking as shown in figure 1.2 (a). The first three models have been observed in T-junction, co-flow and flow focusing geometries. The last two models have not been reported in T-junction yet. In principle,

droplets generated with squeezing mode is larger than the channel dimension and highly monodisperse and dripping mode is smaller than the channel dimension and monodisperse. In the case of jetting, droplets are polydisperse. The droplets in tip-streaming can be as small as submicrometer-scale and monodisperse. The droplets in tip-multi-breaking are polydisperse but geometric-progression size distribution. Transitions between different modes can be achieved by changing the dispersed and/or the continuous phase capillary numbers (Figure 1.2 (b). For example, the squeezing–dripping transitional regime occurs at an intermediate continuous phase capillary number between squeezing and dripping [24].

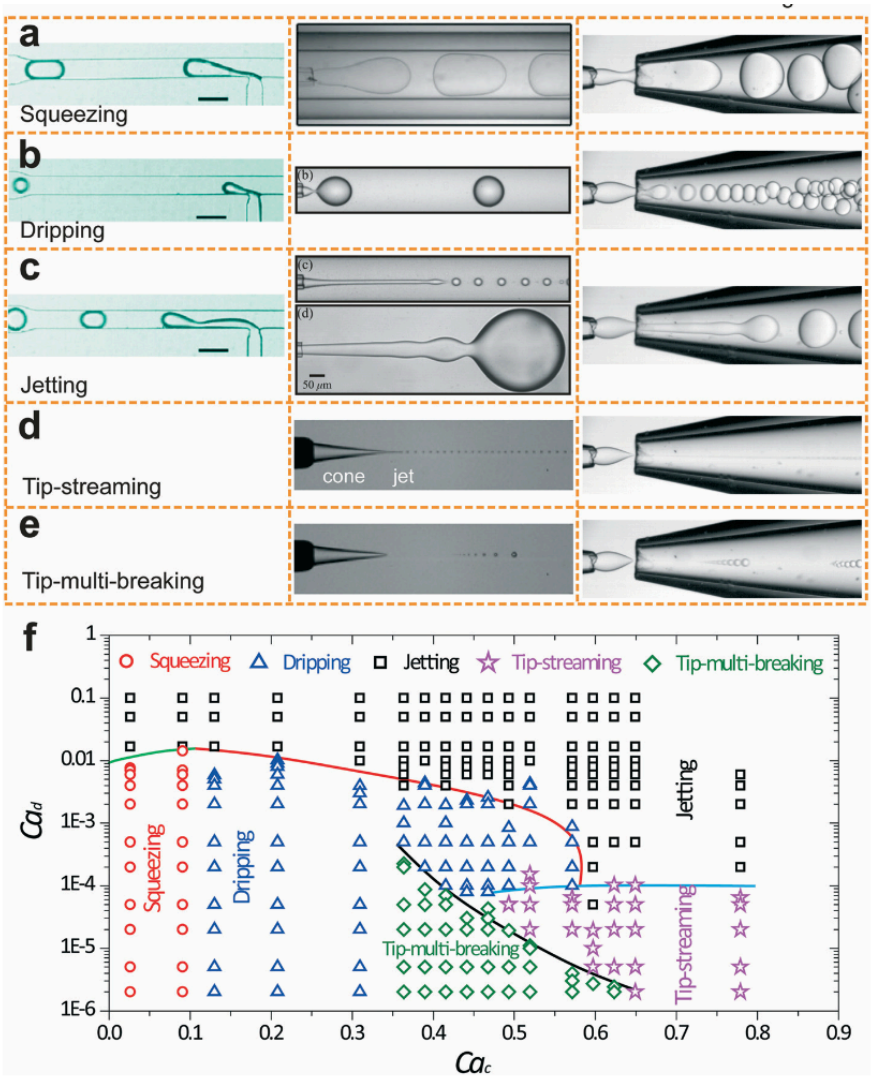

Figure 1.2 Images droplet generation with 5 different modes in T-junction, co-flow and flow focusing geometry. (a) Squeezing mode. (b) Dripping mode. (c) Jetting mode. The upper image in co-flow is a narrowing jet while the lower one is a widening jet. (d) Tip-streaming mode. (e) Tip-multi-breaking mode. Neither tip-streaming nor tip-multi-breaking modes has been reported in cross-flow geometry yet. (f) Phase diagram in capillary number of continuous phase and disperse phase (Ca_c, Ca_d) plane for various modes observed in flow focusing geometry [24].

1.3 Labelling Technologies of the Droplet

For the multiplex assay with the droplet, each droplet should have its identification code to know its content. There are two types of encoding method. One is spectral encoding that incorporates mixtures of luminescent material such as fluorescence dyes or quantum dots, and the another is positional encoding that recognizes geometrical position of each droplet in microfluidic device.

1.3.1 Spectral encoding

Spectral encoding method of the droplet incorporates mixtures of luminescent materials such as fluorescence dyes of quantum dots (QDs) [3, 10, 25-35]. Each luminescent material has individual excitation and emission wavelength, which enables to identify its spectrum [3, 30]. By adjusting mixing concentrations of the dyes, various spectral code can be generated. However, their practical coding capacity of spectral encoding is limited by a few technical challenges. The organic fluorescence dyes have broad emission spectrum, which makes it difficult to decode combination of multiple fluorescence dyes because of spectral overlap. Although the quantum dots have relatively narrow emission spectrum, re-absorption loss limits coding capacity when their concentration is high [32].

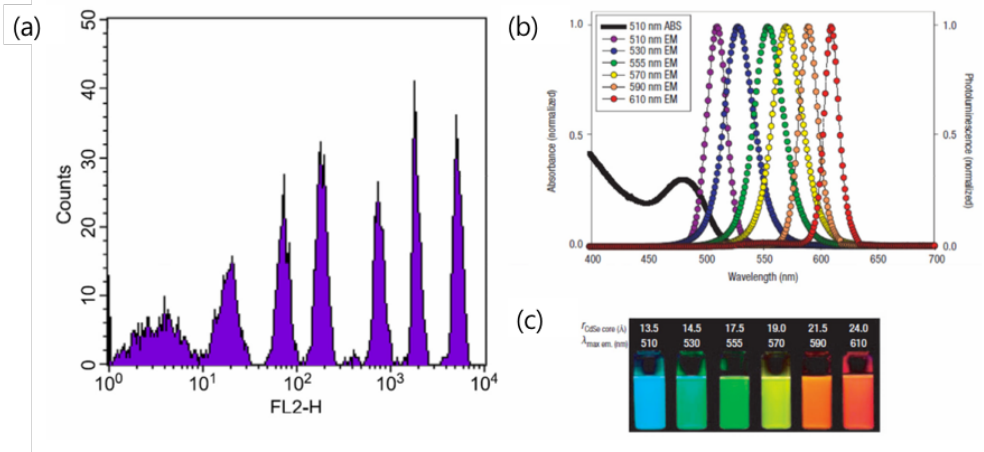

Figure 1.3 Spectral encoding. (A) Fluorescence intensities containing six different quantities of a fluorescence dye. Each dye has distinguishable emission peak of wavelength. (B) Absorption spectrum (black dot) and emission spectrum (color dot) of six quantum dots. (C) Fluorescence emission of quantum dots [36]. By adjusting mixing concentrations of the dyes, various spectral codes can be generated.

1.3.2 Positional encoding

Positional encoding, also called spatial indexing, is widespread method for indexing large number of different molecules in array type platforms such as 96, 384 wellplate or microarrays. This method utilizes x-y coordinate or index of each molecule in the substrate as a code. In droplet microfluidics, each droplet is dispensed to spatially designated spot of array [16, 37-48]. These spatially defined droplet arrays have advantages specially in monitoring time-course profile of each reaction of droplet.

However, in the case of multiplex assays, the position of each spot of microarray or microwell should represent different droplet and each droplet should be dispensed serially with accurate positional registration. Also, sophisticated liquid handling equipment such as inkjet printers or ultrasound nozzles make production of droplet array to be time consuming and expensive.

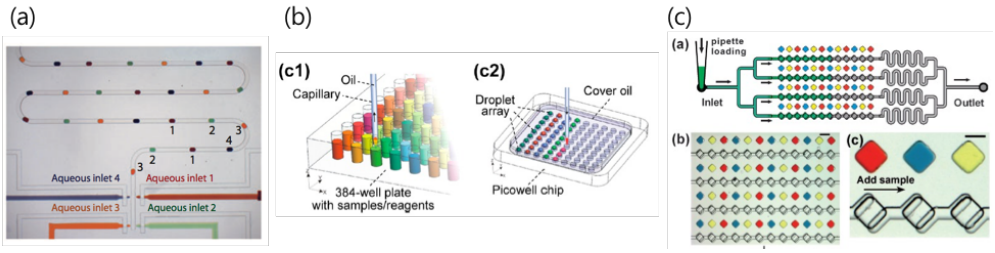

Figure 1.4 Positional encoding of droplets. (a) One-dimension positional encoding of the droplet [49]. (b, c) Two-dimension positional encoding of the droplet. In Two-dimensional encoding, each droplet is serially dispensed with capillary or liquid dispenser [39, 40]. The 1-D and 2-D positions of droplets are indexed for code of the droplets.

1.4 Main Concept

Impact of the droplet microfluidics is already obvious in some applications, at present, the droplet microfluidics is used to analyze thousands of aliquots of a single type of analyte solution. However, there are few methods to process different analytes. The main reason is that unlike common macroscale liquid carriers such as tubes and wells, which can be easily labeled to know their contents, the droplets are difficult to be labeled. To allow the droplet microfluidics with many different type of analytes for multiplex assay, it would be necessary to label the droplets with a number of identification codes. Although a few droplet-encoding methods exist as introduced above, all of these methods could not satisfy both of high encoding capacity and parallel manipulation of droplets.

In this dissertation, I introduce ‘encoded microcapsule’, developing a novel labelling method and a multiplex assay platform for the droplet microfluidics. Just as labeling of tubes in macroscale, microscale graphical codes can be lithographically written on the nanoliter droplets. This approach enables versatile way of storing and processing chemical libraries in highly multiplexed manner. The encoded microcapsule, as a microscale “liquid tube”, encapsulates nanoliter-scale droplets in a solid Teflon shell. Uniquely, a graphical code written on the shell represents the identity of the encapsulated liquids. Since the liquid are completely sealed and encapsulated in a Teflon shell, they do not mix or interact with each other. Therefore,

large number of different microcapsules can be stored in a tube as a pooled chemical library.

For the multiplex assay, these pooled libraries of encoded microcapsules are simultaneously self-assembled into empty microwells in a single pipetting step, eliminating the labor-intensive serial dispensing process to aliquot liquids into the microwells. The graphical codes on the microcapsules can be used to identify each liquid in the microcapsules even when they are randomly positioned in the microwells. The self-assembly of thousands of microcapsules takes only a few seconds, which is equivalent to thousands of serial dispensing steps requiring a few hours. After assembly, each microwell is isolated using immiscible liquid to prevent cross-contamination and evaporation.

The microcapsules are then ruptured by external force such as laser illumination or mechanical squeezing to release the liquid. Next, these liquids can freely react with cells or other floating reagents in the microwell. To show the feasibility of the concept, various liquid phase assays including enzyme inhibitor screening, virus transduction, and drug-induced apoptosis tests are demonstrated. This platform enables multiplex and parallel assays to be conducted in a high-throughput manner regardless of the size of the chemical library.

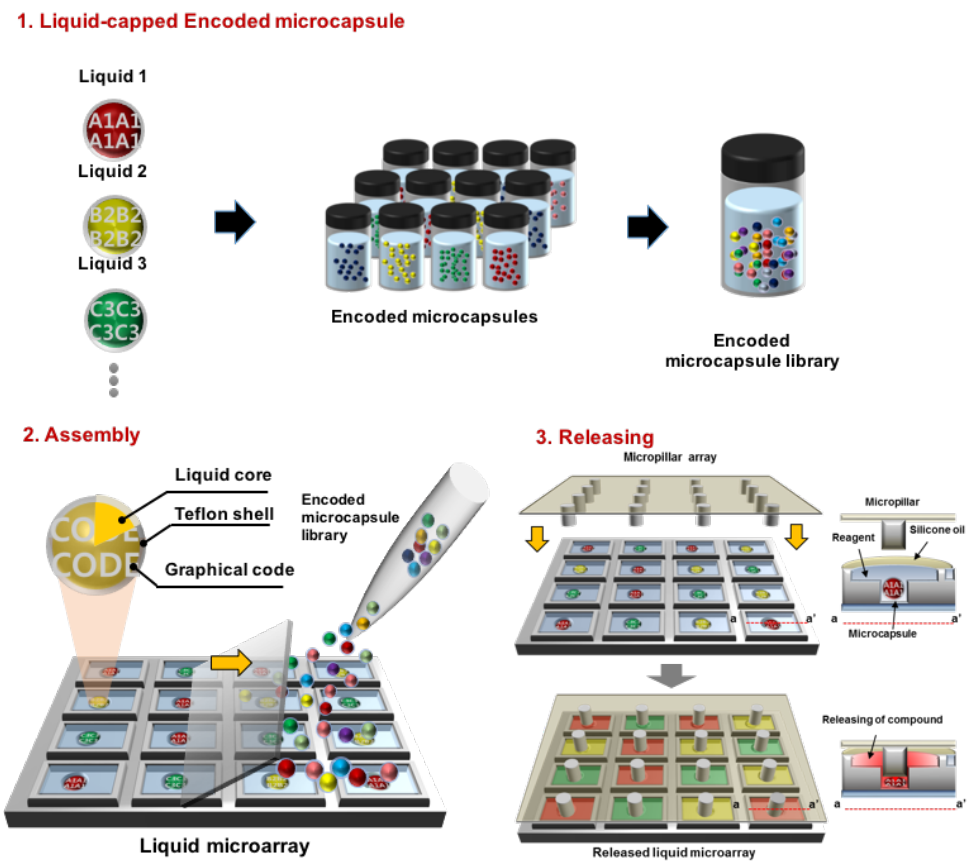

Figure 1.5 Main Concept of this thesis. Various liquid compounds are encapsulated in the solid Teflon shell and the graphical code are engraved on the Teflon shell by lithographic process. These encoded microcapsules are merged together to make encoded microcapsule library. These microcapsules are then self-assembled in the microwell array with a single pipetting step. Various compounds encapsulated in microcapsules were released by applying the releasing cue on the microcapsules and each released compound reacts with liquid or cells in the each microwell.

Chapter 2

Generation of the Liquid-Capped Microcapsule

In this chapter, I introduce process for generation of liquid-capped microcapsule. For generation of the microcapsule, microfluidic device is fabricated by soft-lithography technology. The microfluidic device is chemically treated for hydrophilic surface modification. Double emulsion droplet is generated by flow rate control of the microfluidic device and photo-curable Teflon shell phase of the double emulsion is polymerized by UV exposure. Properties of the microcapsule were analyzed by leakage test, off-centering measurement and long-time storage test of the liquid inside the microcapsule.

2.1 Process for generation of the liquid-capped microcapsule

For generation of the solid microcapsule material, I employed a microfluidic device and photo-curable and solvent-resistant Teflon material, perfluoropolyether (PFPE) (Figure 2.1). The photo-curable PFPE consists of PFPE backbone, urethane block, and UV curable methacrylate end-group. The PFPE, a type of liquid Teflon, is chemically and biologically inert and is highly flexible [50-54]. Also, it is known to have hydrophobic and lipophobic property concurrently, which enables to encapsulate both hydrophilic and hydrophobic compounds with low leakage property [55].

To make the liquid-capped microcapsule, I used microfluidic device generating water-in-oil-in-water (W/O/W) double emulsion droplet by 3D coaxial flow with simple hillock structure [56]. To produce water-in-oil-in-water (W/O/W) double emulsions in the microfluidic channel, the outer path for the outer water phase needed to be hydrophilic. However, the PDMS channel was hydrophobic. So, the microfluidic device is treated to have partially hydrophilic surface by selectively hydrophilic coating. Using the surface-treated microfluidic device, water/PFPE/water double emulsion droplets are generated. The end of microfluidic channel is connected to UV exposing area where the photo-curable PFPE phase of the double emulsion droplet is photo-polymerized and microcapsules are generated.

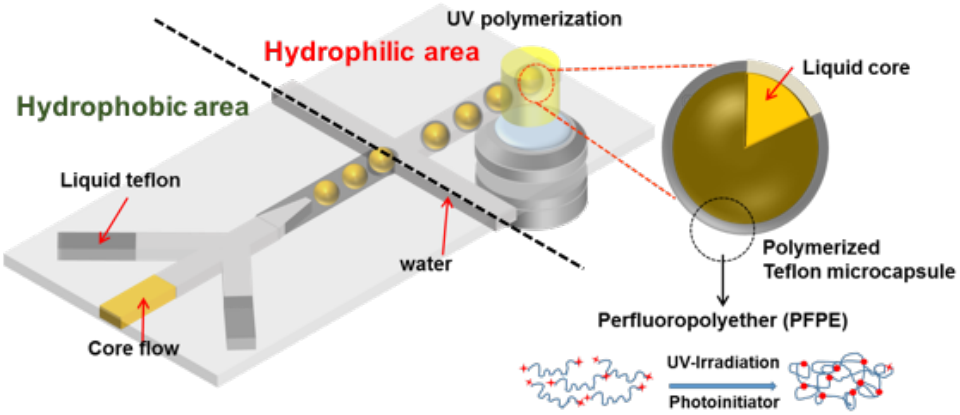

Figure 2.1 Generation of the encoded microcapsule. (A) Schematic image for generation of the microcapsule. Double emulsion droplets of water/PFPE/water are generated by conventional microfluidic devices. After exposure to UV light. The UV-curable PFPE is polymerized and the core liquid is encapsulated by solid Teflon shell.

2.2 Fabrication of Microfluidic Device

Microfluidic device for generation of the liquid-capped microcapsule is fabricated by conventional soft-lithography technique. Here, I employed a PDMS microfluidic device that had a hillock structure for generating double emulsion droplets. The microfluidic device generates a three-dimensional coaxial flow by adding a simple hillock to produce alginate core-shell microcapsules to efficiently form cell spheroids [56].

The microfluidic channel with a hillock structure was made via a multi-level SU-8 fabrication method and a PDMS replica molding process. First, masks for the channel were drawn using AutoCAD software. One mask was for the hillock and the other mask was for the channel. The channel width was 200 μm, and the angle between the edges of the hillock was set to 60°. A mold for the microfluidic channel was produced using the two masks and an SU-8 negative photoresist. The SU-8 photoresist was poured onto the silicon wafer and spun. The spin speed was set to have a microstructure with a height of 25 μm. This structure was the first layer. After irradiating the mask for the channel with patterned light, the first layer with a height of 25 μm was produced. The second layer for the hillock was produced by pouring the photoresist onto the first layer and selectively curing the second layer. Subsequently, the unpolymerized photoresist was removed using developing solution, and the microfluidic channel mold was finally produced.

The PDMS channel with a hillock structure was produced by PDMS using the SU-8 mold. The silicon wafer, which has an SU-8 channel mold, was attached to a glass dish by a transparent tape. Then PDMS (Sylgard 184; Dow Corning, Midland, MI) was mixed with the curing agent at a volume ratio of 10:1. This mixture was poured onto the SU-8 channel mold, and the solution was degassed in a vacuum chamber for 30 min. The solution was heated on a hotplate at 150 °C for 15 min. The PDMS slab was peeled off from the SU-8 mold and cut into several PDMS microfluidic channels. The complete PDMS microfluidic channel with a hillock structure requires the combination of two microfluidic channels. Therefore, two PDMS channels were treated with oxygen plasma for 1 min, and then the channels were combined under a microscope.

To produce water-in-oil-in-water (W/O/W) double emulsion droplets, the outer path for the outer water phase needed hydrophilic surface treatment because the PDMS surface is hydrophobic. The PDMS channel surface was made hydrophilic as follows. First, the two slabs of the PDMS channel with a hillock were prepared. Holes for the inlets and outlets were created, and the slabs were washed with ethanol and dried with nitrogen gas (N2). Then, the PDMS slabs were treated with oxygen plasma for 1 minute (CUT-MP, Femto Science). Before the hydroxyl groups of the PDMS surface disappeared, two slabs were attached to form one united channel with a height of 200 μm under a microscope. The bond between the two slabs was strong enough to

allow the flow of liquids inside the channel. The bonded slabs were attached to a glass slide. Within 5 minutes, the silane coupling agent, 2-[methoxy(polyethyleneoxy)-propyl]trimethoxysilane (Gelest) in toluene (at a volume ratio of 9:1) was introduced into the assembled channel using a suction equipment for 20 seconds. The solution residues and bubbles cause non-uniform surface modification. When the reaction solution was introduced into the channel with the suction equipment, the residues and bubbles were effectively removed. Moreover, the suction equipment allowed selective surface modification of the PDMS channel because the strong suction prevented liquid overflow from the outside into the hillock side. The channel was then left at room temperature for 5 minutes under pressure. The toluene was poured into the channel for several seconds, and the channel was washed with ethanol for 30 seconds. Channel bonding was maintained during the flowing process of these several liquids. Finally, the channel was heated on a hotplate at 100 °C for 10 minutes (Figure 2.2).

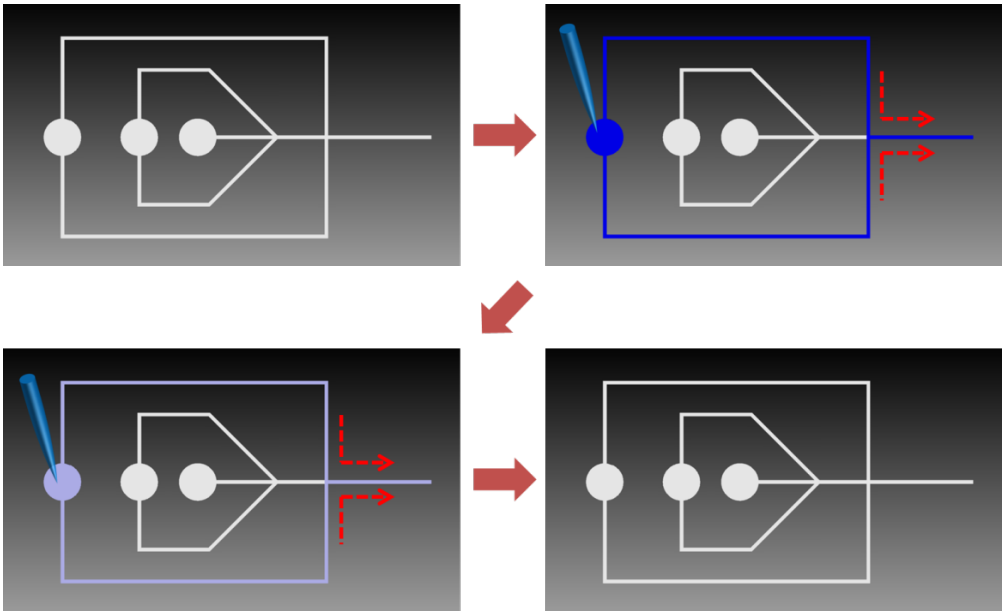

Figure 2.2 The schematic of PDMS surface modification. After plasma treatment and bonding of two PDMS channel, the channel is treated with the silane coupling agent and washed with toluene and ethanol sequentially. Blue color represents treatment of the silane coupling agent and violet color prevent washing process with ethanol.

2.3 Generation of the Double Emulsion Droplets

The liquid-capped microcapsules are fabricated by photo-polymerization of the middle phase of the double emulsion droplets that are generated with microfluidic device. After selectively hydrophilic coating of the microfluidic device, deionized (D.I) water with 2% surfactant (BSSF), is introduced in the outer phase to wet the whole surface of the microfluidic channel. Then, the photo-curable perfluoropolyether (PFPE) with 3wt% photoinitiator (DMPA) is introduced in the middle phase. The concentration of the photoinitiator is chosen to minimize cytotoxic effect of the photoinitiator to the cells. After that, the aqueous liquid is introduced in a core phase. The aqueous liquid in the core phase is introduced in the hillock microfluidic channel. When the aqueous liquid meets the PFPE in the middle phase, the aqueous liquid forms the coaxial flow by shear stress between aqueous liquid and PFPE, and passes the hillock structure with along with PFPE. In the slanted region of hillock structure, the PFPE in middle phase break the coaxial aqueous liquid stream and make aqueous liquid droplets that flow within the PFPE phase. At the cross-junction where the PFPE in the middle phase and D.I water in the outer phase meet, the D.I water in the outer phase cut the PFPE phase containing aqueous droplet and generated aqueous liquid/PFPE/D.I water double emulsion droplets, as shown in Figure 2.3.

These double emulsions pass through the outlet of the channel and flow through tube which is connected with outlet of the microfluidic channel. The double emulsion

droplets in the tube are exposed to UV light. The PFPE in the middle phase of the double emulsion droplet is polymerized UV light and the solidified PFPE microcapsule encapsulates aqueous liquid of the core phase. After UV exposure, polymerized PFPE microcapsules are gathered in a bottle containing water with surfactant to prevent aggregation. For visualization, I mixed green fluorescence dye (FITC) in water phase of the double emulsion droplets. Figure 2.3 (b) shows that the collected PFPE microcapsules containing green fluorescence dye in the core liquid. By comparing results before and after breakage of the microcapsules, I observed that the PFPE microcapsules can stably encapsulate inner fluorescence dye liquid.

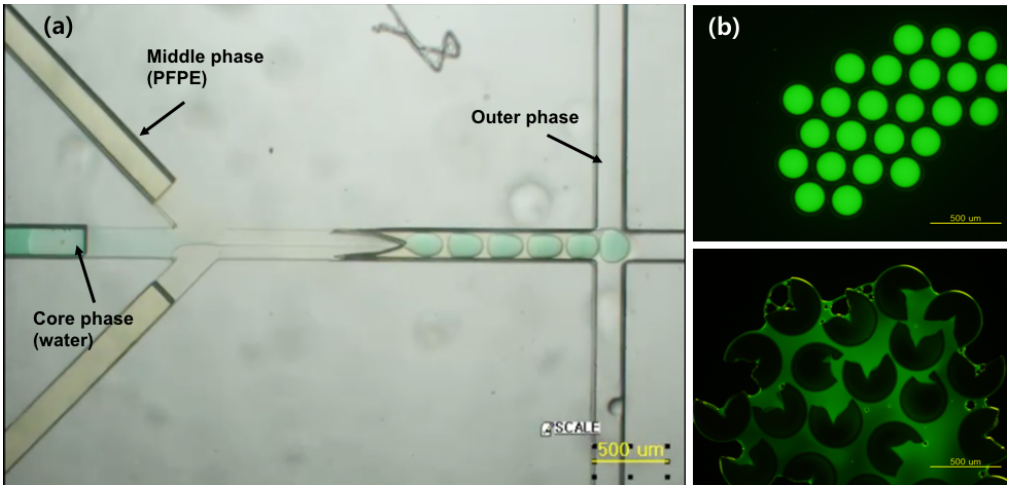

Figure 2.3 Generation of water-PFPE double emulsions in the surface-modified PDMS microfluidic channel with the hillock structure: (a) Fabrication of PFPE double emulsions in the hillock channel. Core phase water flow and Middle phase PFPE flow meet and generate water droplet.

At cross-junction, Outer phase water flow break the water-in-PFPE droplets and generate water-PFPE-water double emulsion droplet (b) Fluorescence images of polymerized microcapsules containing green fluorescence dye before and after breakage. Gathered PFPE microcapsules stably encapsulate inner fluorescence dye liquid before breakage.

As the polymerized PFPE is chemically and biologically inert, various liquids can be encapsulated. For visualization, I made 9 different microcapsules which containing 9 different colored food dye (Figure 2.4 (a)). Each kind of the microcapsules are generated using the microfluidic device and stored in each bottle. Then, the microcapsules in all bottles can be mixed together in a bottle to make a microcapsule library as shown in figure 2.4 (b, c).

The polymerized PFPE is also physically flexible. As shown in figure 2.4 (d), even the microcapsules are squeezed in some degree with micro tweezers, they are not burst and return back to their spherical shape after squeezing. As the microcapsules preserved stably without cross-contamination when they are mixed together. It enables user to easily generate microcapsule library and to handle various microcapsules in parallel for self-assembly of the microcapsules, which will be described later.

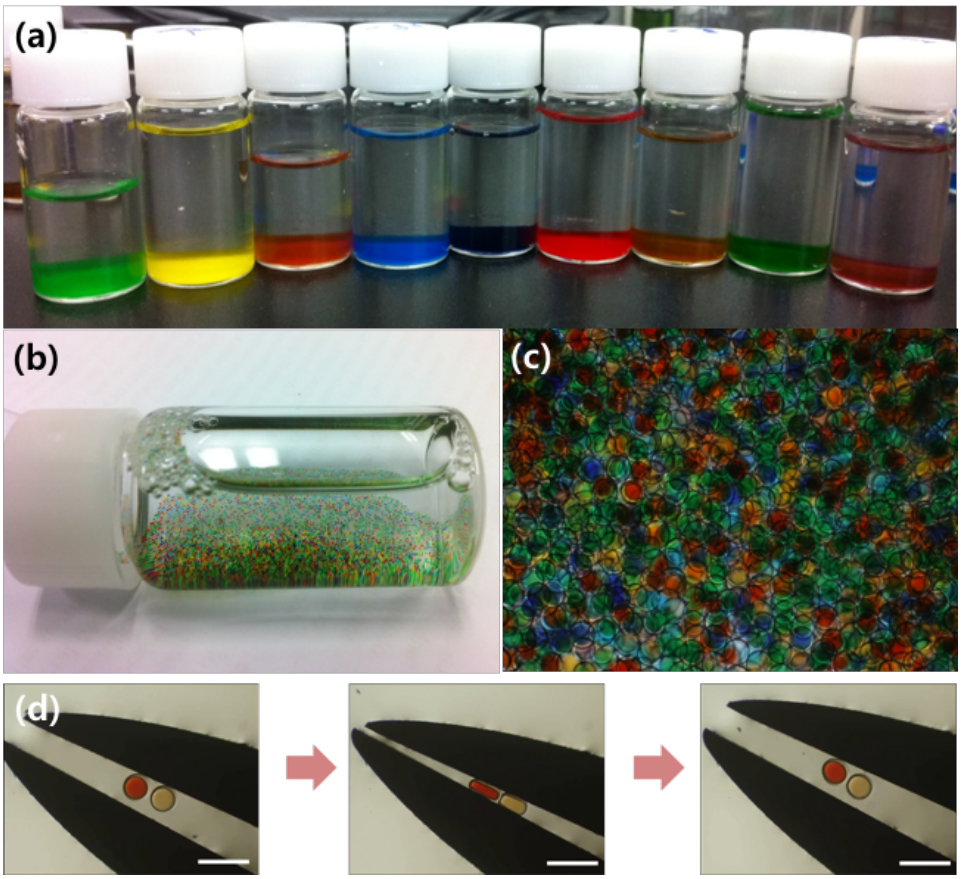

Figure 2.4 Generation of liquid-capped microcapsule library. (a) 9 different microcapsules that containing 9 different colored food dye. (b, c) All kinds of microcapsules are mixed in a bottle and make a microcapsule library. (c)High flexibility of polymerized PFPE microcapsule. As the PFPE is chemically and biologically inert, various liquid can be encapsulated and preserved stably without cross-contamination when they are mixed together. The scale bar is 400 μm.

2.4 Flow-rate Control for Generation of Double Emulsion

In order to find suitable flow rate condition for generation of microcapsule, I varied either core or outer phase flow rate by fixing the other flow rates. In low outer flow rate (outer flow rate < 3000 μl/hr.), double-core emulsions are generated because outer flow rate is not sufficient to break the middle phase to have only one core phase droplet. In middle range flow rate of the outer flow (3000 μl/hr < outer flow rate < 5000 μl/hr), normal single core double emulsion droplets are generated. In high outer flow rate (outer flow rate > 5000 μl/hr), satellite drops are generated because the outer phase breaks the middle phase before the entire core phase droplet pass the junction of the channel.

In low core flow rate (core flow rate < 30 μl/hr), it leads to multiple drops in PFPE droplet (Figure 2.5 (a)). In this flow region, generation mode of the core droplet changes from dripping to jetting. As I increase the core flow rate (core flow rate > 30 μl/hr), single core double emulsion droplets are generated by changing generation mode from jetting to dripping and diameter of the core droplet is increased and thickness shell is decreased. Here, size of double emulsion droplet is not significantly increased because the size of droplet is mainly affected by dimension of microfluidic device. At high core flow rate (core flow rate >270 μl/hr), the thickness of shell is too thin as the diameter of the core liquid increase, and the double emulsion droplets are unstable and core liquid is burst (Figure 2.5 (b)).

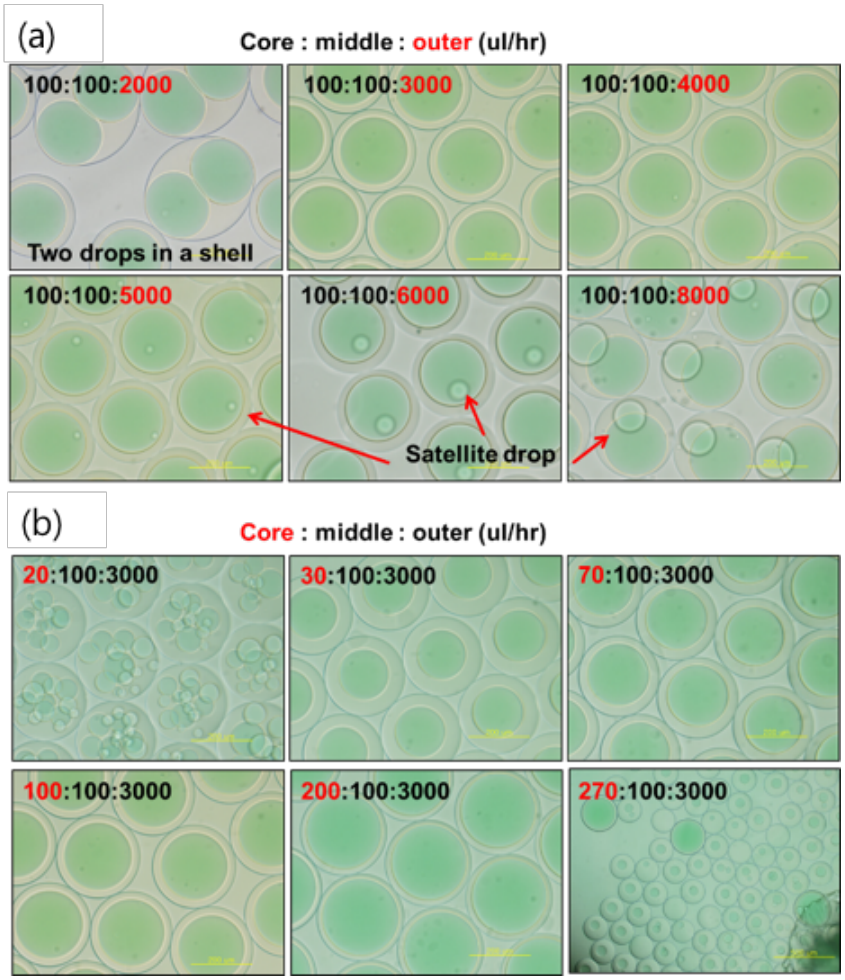

Figure 2.5 Flow rate control results. (a) Outer flow rate control results. The flow rates of the other phases are fixed. In high outer flow rate, satellite drops are generated because outer phase break the middle phase before entire core phase droplet pass the junction of the channel. In low core flow rate, it leads to multiple drops in PFPE droplet because the outer flow rate is too slow to break one core phase droplet. (b) Inner flow rate control results. As I increase the core flow rate, diameter of core drop is increased and thickness shell is decreased. At high core flow rate, the thickness of shell is too thin and core liquid is burst. Size of double emulsion droplet is not significantly increased.

Using the microfluidic device and controlling the flow rates, I can obtain uniform size of droplet as shown in figure 2.6. To measure the diameter of the core liquid, I mixed green fluorescence dye in core liquid. After generation of the microcapsule, fluorescence image of the microcapsule is analyzed with image processing program by Matlab and the histogram of diameters of the core liquids is obtained as shown in figure 2.6 (b). From the histogram, I observed that average diameter of the core liquid is 182.65μm and CV is 3.08%.

The generation frequency can be calculated from the flow rate of the core liquid, because the core liquid is only used for the core of the microcapsule. By dividing the flow rate of core liquid to the volume of the core liquid in the microcapsule, the generation frequency can be obtained. In my experiment, flow rate of the core liquid was set to 200 μl/h and measured volume of the core liquid in the microcapsule was 4.2 nl. Theoretically, the generation frequency of the droplets is about 47600 droplets/hr.

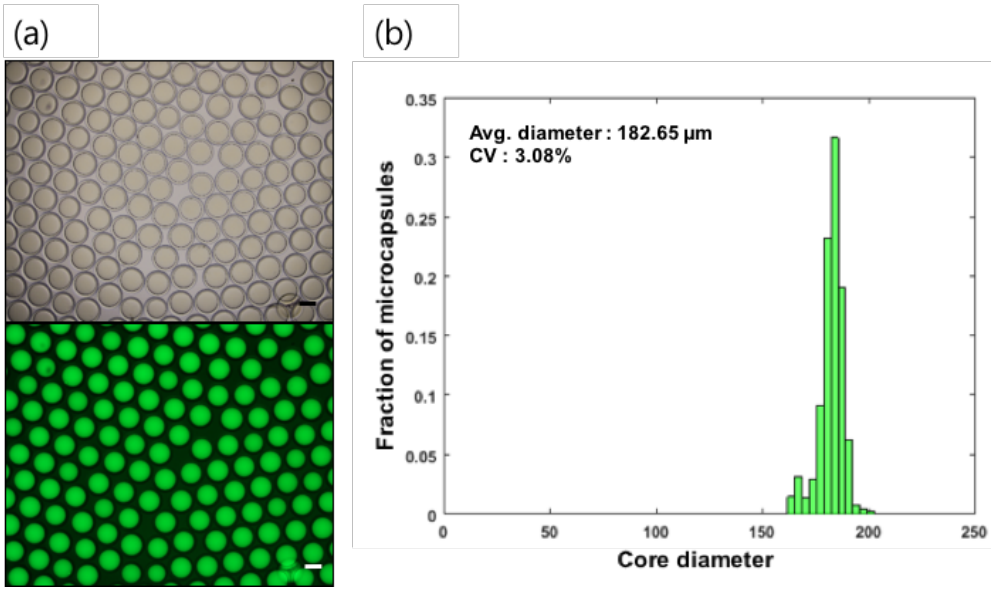

Figure 2.6 Uniform diameter of the core liquid enables to control volume of the liquid precisely. Average diameter of the core liquid of the microcapsule is 182.65 μm and CV is 3.08%. The generation frequency can be calculated by dividing the flow rate of core liquid to the volume of the core liquid in the microcapsule, which is about 47600 droplets/hr.

2.5 Photopolymerization of the Double Emulsion Droplets

After the core liquid droplets are generated by PFPE/initiator mixture, outer water breaks the core-containing PFPE phase, which generates double emulsion droplets. The PFPE polymer is polymerized by UV irradiation (wavelength: 365 nm, 50mW/cm^2) for 10 seconds and the core liquid is encapsulated by a polymerized PFPE microcapsule. In previous work of Vitale and coworkers [54], polymerization kinetics of PFPE was studied by three different techniques, FT-IR analysis, DSC analysis and insoluble fraction measurement. They proved that the conversion of polymerization reaches 100% at about 60 seconds of UV irradiation at 3mW/cm^2. In my experiment, the FT-IR analysis of polymerized PFPE according to various UV exposure time was performed to identify the extent of polymerization. It is known that as the PFPE is polymerized, the absorption peak at 1638 cm^{-1} disappears. The figure 2.7 shows that the absorption peak at 1638 cm^{-1} decrease as UV exposure time increase until UV exposure time of 25 seconds. In longer UV exposure time than 25 seconds, there is no significant change at the absorption peak. From the FT-IR results, I can conclude that the PFPE is fully polymerized more than 25s of UV exposure time at 15mW/cm^2.

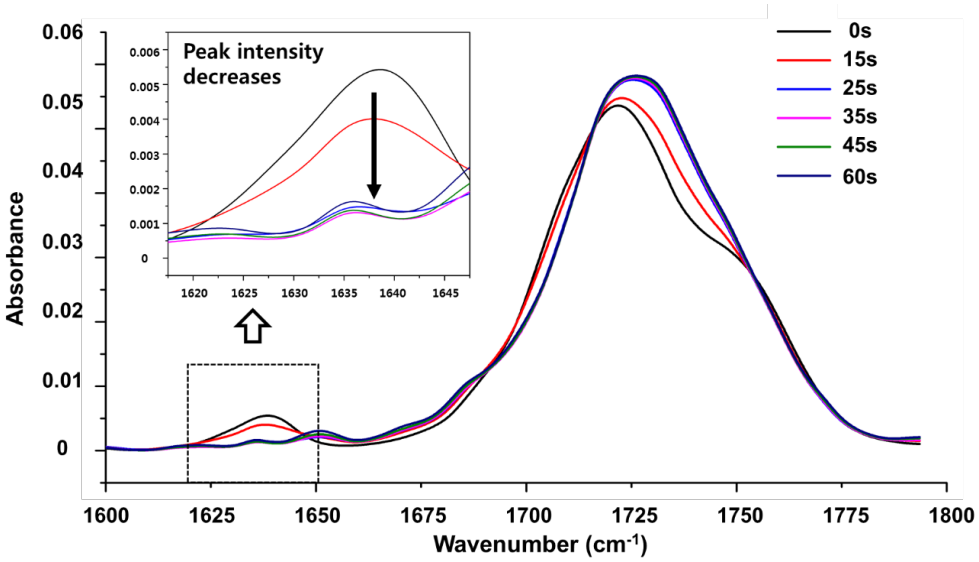

Figure 2.7 FT-IR analysis of polymerized PFPE according to various UV exposure time. PFPF with 3wt% of DMPA is polymerized at different exposure time (from 0 to 60s) at 15mW/cm^2. Conversion of PFPE monomer to polymer is observed by monitoring methacrylate C=C peak at 1638 cm^{-1}. PFPE is fully polymerized more than 25s of UV exposure time.

2.6 Properties of the Microcapsule

2.6.1 Leakage Test

For generation of a pooled microcapsule library, it is necessary that the core liquid should be stably sustained inside the microcapsule for a long time until they are used. To verify stability of encapsulation, microcapsules containing fluorescent dye (Fluoroscein, Sigma-Aldrich) was fabricated and assembled in the microwell array. After assembly, the microwell was sealed by slide glass and fluorescent intensity of surrounding liquid in the microwell was monitored for a month. For a comparison, a microcapsule in one microwell was broken and the fluorescent intensity of released fluorescent dye was measured (red dot line). The measured fluorescent intensities are shown in figure 2.8. The graph shows that there is almost no leakage from microcapsule and the core liquid is stably encapsulated by polymerized PFPE shell for a long time.

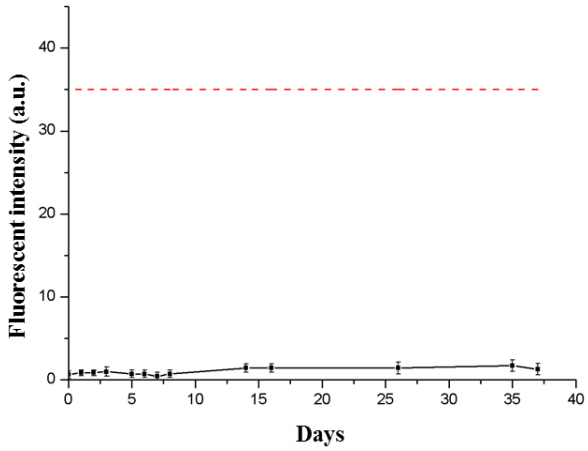

Figure 2.8 Results of leakage test. Fluorescent intensity of surrounding liquid in the microwell. Microcapsule containing fluorescent dye (fluorescein) was assembled in each microwell and the fluorescent intensity was measured for a month. Red dot line represents reference intensity when the microcapsule was broken and the fluorescent dye in microcapsule was released in the microwell.

2.6.2 Off-centering of the Microcapsule

I observed that after the assembly of microcapsules, the thicker part of shell on each microcapsule faced downward. When a double emulsion droplet is generated, there is buoyant force corresponding to the density difference between the core and middle phases. The force causes a core drop to be raised before polymerization [57, 58], making off-centered double emulsion droplet. After polymerization, microcapsules exhibit inhomogeneous shell thicknesses. During assembly, the microcapsules are rotated and thicker part of shell is faced downward, which minimize

gravitational potential energy of the microcapsule. To clarify an effect of inhomogeneous shell of microcapsule to the assembly, I observed cross section view of assembled microcapsule.

To observe cross section of the microcapsule, microcapsule should be fixed in their status after assembly. So, I exchanged stock solution of microcapsules to photo-curable PEG-DA solution. I diluted the PEG-DA with D.I water to decrease viscosity of solution and enables the microcapsules to move freely during assembly process (PEG-DA: D.I water = 1 : 20). After assembly of the microcapsules, the PEG-DA solution is cured by UV light and cured PEG-DA is detached carefully from the microwell array. The microcapsules are trapped in cured PEG-DA layer and by slicing the PEG-DA layer, I observed cross-section view which show off-centered microcapsules in microwell (Figure 2.9). By utilizing this off-centering property through encoding at the thicker part of shell, I can easily recognize each code and its contents of the microcapsule after assembly in the microwell.

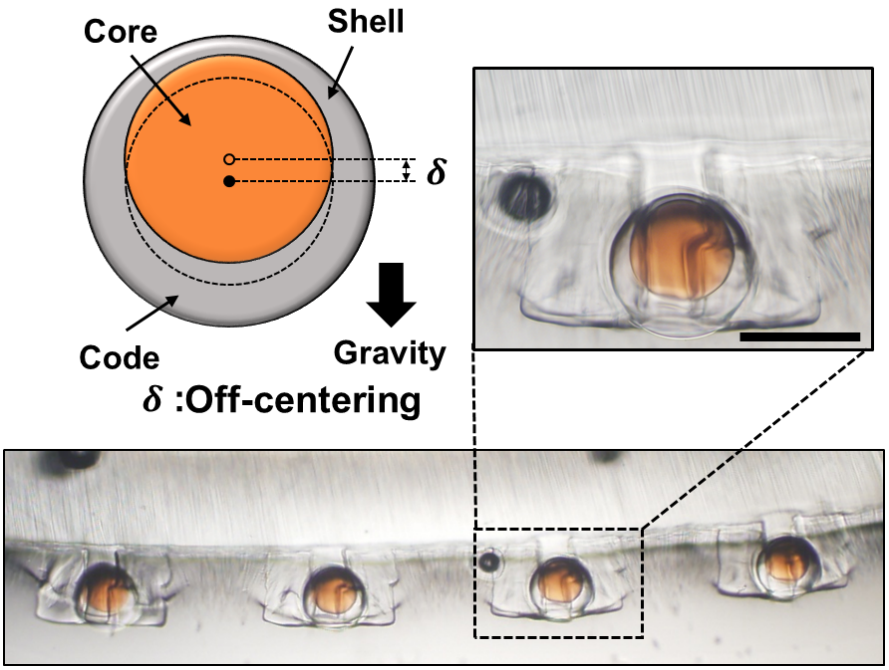

Figure 2.9 Off-centering feature of the microcapsule. The images show cross-section view of the microcapsules assembled in the microwells. The microcapsules rotate during assembly process to minimize gravitational potential energy and thicker part of shell faces downward, which has advantage in encoding and decoding process.

2.6.3 Long Time Storage Test of the Liquid inside the Microcapsule

To verify stability of core liquid inside microcapsule, long time storage test is also conducted to identify whether the property of chemical compound in microcapsule remains with the passage of time. I performed simple enzyme-substrate reaction with the β-galactosidase in the microwell and fluorescein-di-beta-D-galactopyranoside (FDG) in microcapsule. Microcapsules containing FDG substrate

are assembled in the microwell with the β-galactosidase. After sealing with immiscible silicone oil, the microcapsules are broken. When the microcapsule is broken and the FDG substrate in microcapsule is released into the microwell, The FDG is sequentially hydrolyzed by β-galactosidase to highly fluorescent fluorescein (Excitation/Emission = 492/520 nm) and the fluorescent intensity was measured according to reaction time (Figure 2.10). The graph shows that the chemical inside microcapsule can maintain its property until 20 weeks.

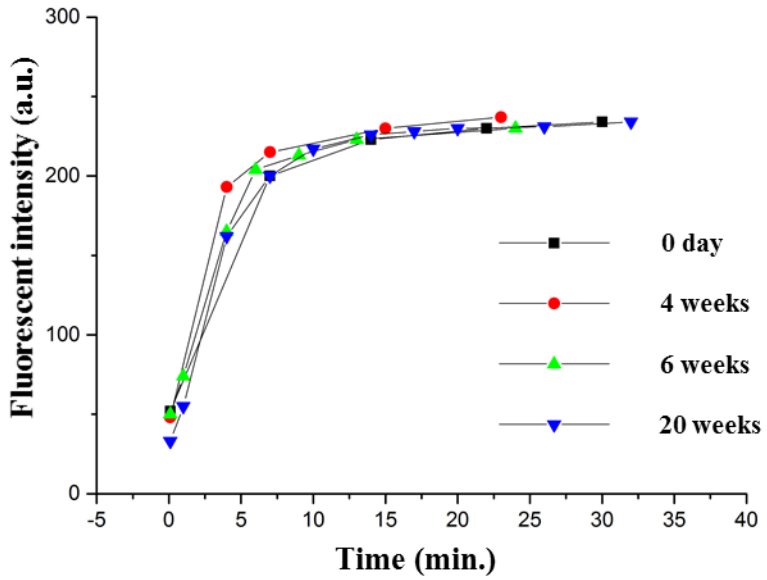

Figure 2.10 Long time storage test according to passage of time. The graph shows that time-course fluorescent intensity of enzyme-substrate reaction according to various storage periods.

Chapter 3

Encoding of the Liquid-capped Microcapsule

In this chapter, encoding method of the microcapsule is described. I found that DMPA photoinitiator mixed with Teflon polymer displayed photoluminescence property after exposure to UV light. Characteristic of DMPA after UV exposure is first analyzed and encoding process utilizing patterned UV light is described. Also, characteristics of graphical code in the microcapsule such as code diversity, variation of fluorescence intensity according to UV light exposure time and DMPA concentrations, and code durability are analyzed. Finally, image processing to recognize code in the microcapsule after assembly is introduced.

3.1 Photoluminescence property of DMPA

3.1.1 Photoluminescence property of DMPA

A key difference between our microcapsule and previously reported is that our microcapsule [55, 56, 59-68] includes a “graphical code” on the shell, allowing for identification of each chemical compound in the microcapsule. To the best of our knowledge, this is the first work to incorporate the graphical code on the microcapsules. Here, I found that a photoinitiator (2, 2-dimethoxy-2-phenyl-acetophenone, DMPA, Sigma Aldrich) mixed with a photo-curable polymer displayed photoluminescence (PL) after exposure to UV light.

To verify that the DMPA has photoluminescence property after UV exposure, I measured fluorescence intensities of six different experimental conditions; PFPE only, PFPE and UV exposure (PFPE/UV), PFPE with DMPA (PFPE/DMPA), PFPE with DMPA and UV exposure (PFPE/DMPA/UV), DMPA only, and DMPA and UV exposure (DMPA/UV). As shown in figure 3.1, only two conditions, PFPE/DMPA/UV and DMPA/UV have fluorescence spectrum at excitation wavelength of 488 nm and the spectrums have similar shape and wavelength peak at 550 nm. The results show that the DMPA appears photoluminescence property after UV irradiation and the fluorescence spectrum has wavelength peak at 550 nm.

Here, I utilized this property of DMPA photoinitiator to encoding of the microcapsule. By applying additional patterned UV light to the PFPE microcapsules

by using a digital micromirror device (DMD) or physical mask, the fluorescent graphical code corresponding to the mask pattern can encoded on the shell of the microcapsule without using special coding materials.

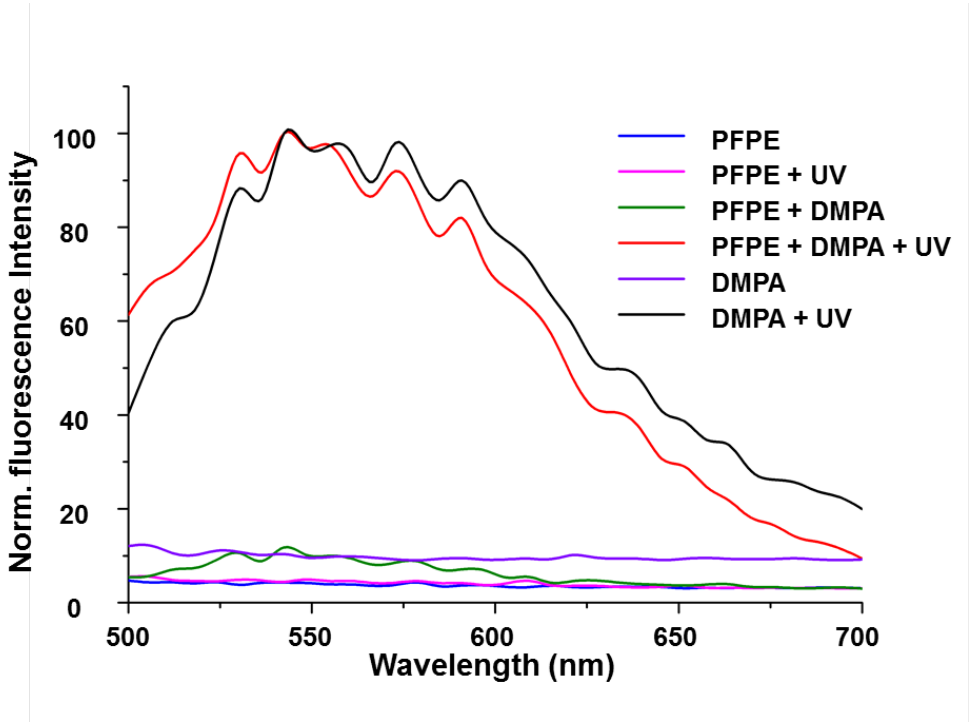

Figure 3.1 Fluorescence intensities of materials within consisting of the microcapsule under various conditions. From the results, I can verify that the DMPA has photoluminescence properties after UV exposure.

3.1.2 Properties of photolysis products of DMPA

To identify that the fluorescence property of the DMPA photoinitiator is came from the photolysis product of DMPA, I extracted photolysis products of DMPA and

measured fluorescence spectrums of the products as shown in figure 3.2 (a). First, PFPE with 3 wt% of DMPA are mixed and photo-polymerized with UV light, and the polymerized PFPE polymer is sliced into small fragments. The PFPE fragments are then immersed and stirred in methylene chloride (MC), and photolysis products are extracted into the MC. After removing solid PFPE fragments from MC solution with filter paper, the photolysis products are extracted by liquid column chromatography and thin layer chromatography. During process of the chromatography, different compounds move down the column at different rates depending on their relative affinity/polarity for the adsorbents and solvent. For example, less polar compounds are easily flow away from the adsorbent and is extracted first. Here, I obtained six different photolysis productions after extraction. Then, each extracted product is analyzed by fluorescence spectrometer to measure fluorescence spectrum of the photolysis product.

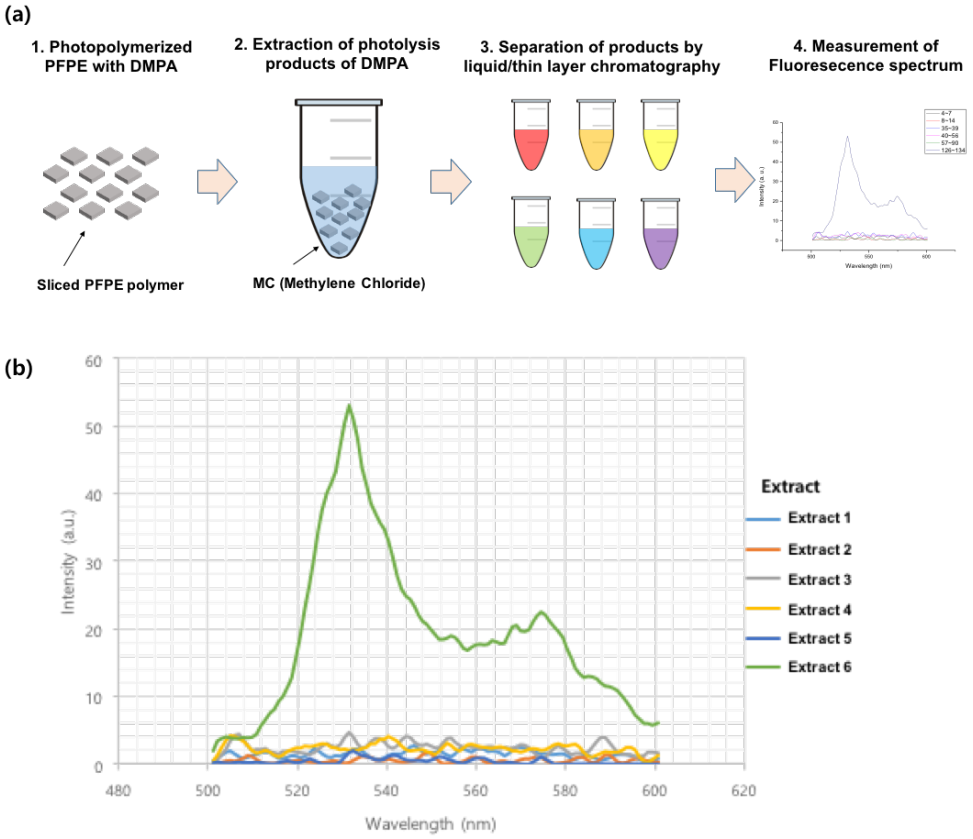

Figure 3.2 Process for measurement of fluorescence spectrum of the photolysis products. (a) Photo-polymerized PFPE is sliced into small fragment and immersed in the methylene chloride solvent to extract photolysis products. After extraction, the photolysis products are separated by liquid/thin layer chromatography. Each separated product is analyzed to measure fluorescence spectrum. (b) Fluorescence spectrums of photolysis products. One photolysis products show similar fluorescence spectrum with fluorescence spectrum of polymerized PFPE.

Among 6 photolysis products, one product (extract 6) show fluorescence spectrum similar with spectrum of polymerized PFPE, which has peak of spectrum at 530 nm wavelength. Other 5 photolysis products (extract 1~5) show no fluorescence signal (Figure 3.2 (b)). I repeated same experiments and the results show similar fluorescence spectrum and wavelength peak at 530 nm (Figure 3.2). From the results, I can conclude that the photolysis product of DMPA show photoluminescence property after UV irradiation.

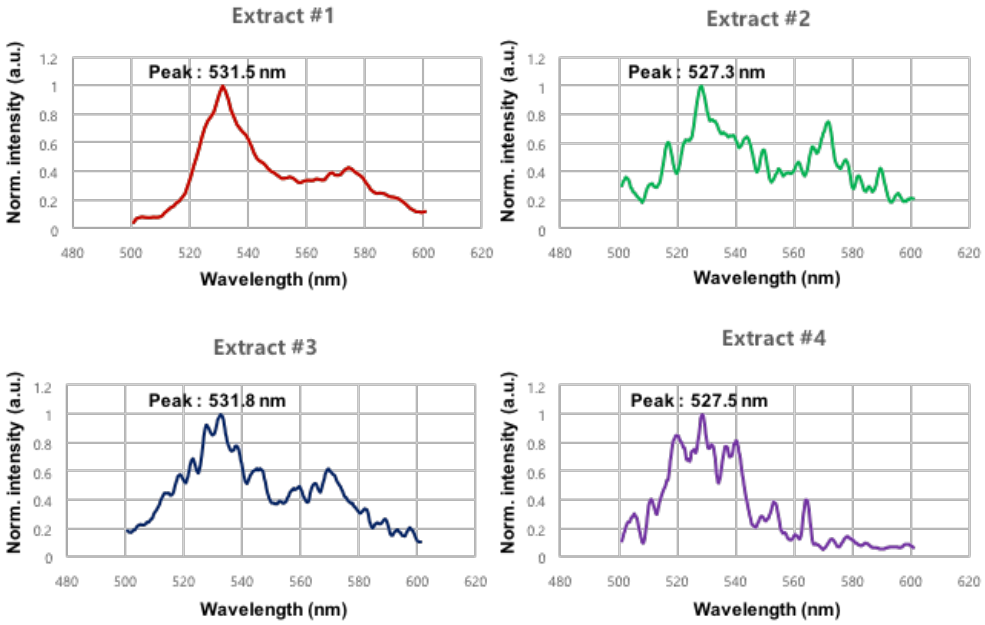

Figure 3.3 Fluorescence spectrums of photolysis products in 4 different experiment. All of the results show similar feature of the spectrums and have wavelength peak at 530 nm.

3.2 Encoding Process

The polymerized PFPE microcapsules are packed on a transparent substrate to consist monolayer of the microcapsules and patterned UV light (wavelength: 365 nm, 180 mW/cm^2) is illuminated on the shell of microcapsule. There are two encoding methods. One is using digital micromirror device (DMD, Texas Instrument, figure 3.4 (a)) and another one is using patterned physical mask (Figure 3.4 (b)). DMD acts as a computer-controlled spatial light modulator and by changing the pattern of the DMD, patterned UV light is illuminated on the microcapsules and various codes can be simply encoded without physical mask.

As another method, the film-combined glass mask (FCG mask, Microtech, South Korea) was used to generate patterned UV light. The patterned film was attached to the glass. The microcapsules were placed on the FCG mask and UV light was illuminated from the bottom of the mask. When the UV light passed through the mask, the opaque parts of the mask blocked the UV light. Thus, the only patterned UV light reached the microcapsules. Considering the illuminated region is not limited to the field of view of the microscope, whole microcapsules on the mask can be exposed to UV light and high-quantity encoding of microcapsules is possible as we increase the size of the mask. In both case, the code areas of polymerized microcapsules were selectively exposed to UV light for 60 seconds and encoded microcapsules were fabricated. The code on the microcapsule did not disappear even in additional UV light

exposure to the entire area (Figure 3.5).

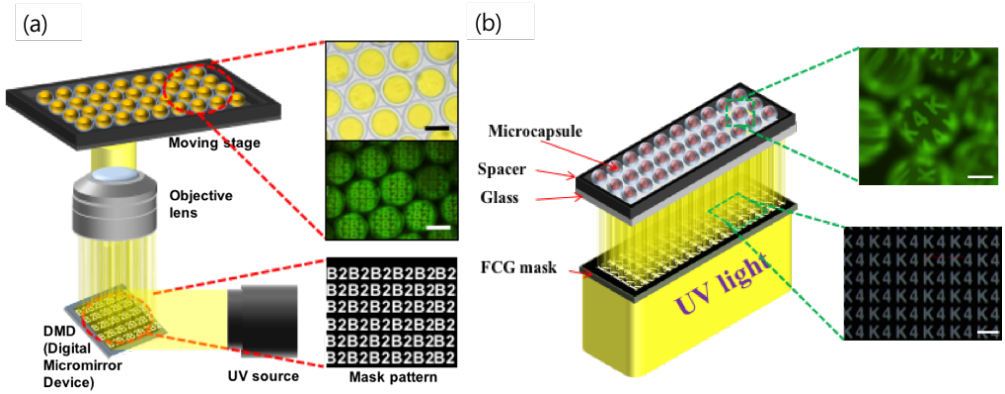

Figure 3.4 Schematic image of the encoding process using (a) digital micromirror device (DMD) or (b) physical patterned mask. Patterned UV light is illuminated to the microcapsule and the pattern is engraved into the shell of the microcapsule.

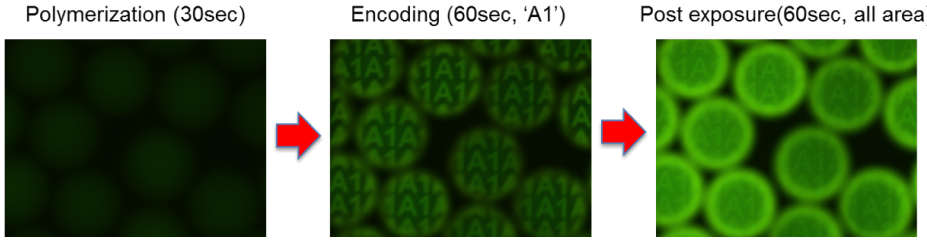

Figure 3.5 Two-step UV light exposure process for encoded microcapsule. To generate encoded microcapsule, microcapsules are first exposed to UV light for polymerization (30sec) and patterned UV for encoding (60sec). The code on the microcapsule exists even in additional UV exposure to entire area (60sec).

Confocal images of microcapsules were captured to verify the presence of fluorescent codes on the microcapsule shells. The microcapsules were 240 μm in diameter. The microcapsules were scanned vertically from the bottom (z = 0 μm) to the center (z = 120 μm) as shown in figure 3.6. Only PFPE shells were observed at the bottom of the capsules so that triangular fluorescent codes were observed without hollow circles. As the scan plane progressed up to z = 20 μm, more codes were observed because the shell regions expanded, but the fluorescent codes at the center of the microcapsule is blurred because focusing is change. At z = 40 μm, the hollow black circular region was observed inside the fluorescent code region, which indicates that the fluorescent codes were only present in microcapsule shells, not in the liquid in the core. As the scan plane moved further, the codes were confirmed to be present only in the shells. The figure 3.6 (c) shows the convoluted three-dimensional fluorescent images of the microcapsules. The triangular code array was in the shells. Code thickness equaled the shell thickness of the capsules.

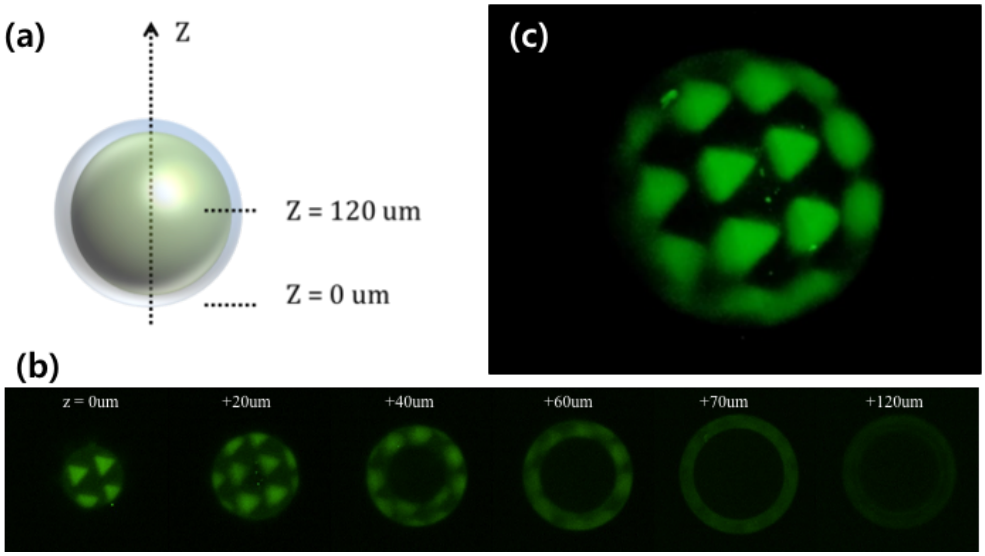

Figure 3.6 Verification of encoded regions of the microcapsules: (a, b) The images of the encoded microcapsule were obtained at different vertical positions with confocal microscopy. (c) Convoluted 3-D image obtained from confocal microscopy. The triangular code array exists only on the shell of the microcapsule.

3.3 Code Variety of the Microcapsule

To represent variety of code of the microcapsule, diverse patterns such as circles, squares, triangles, and hearts were loaded into the software. The UV light patterns were created using the OFML setup. The mask image files are shown in the insets of the figure 3.7 (a). The light patterns were focused onto the PFPE shells of microcapsules through the objective lens. The focal plane was centered on the bottom half of the capsules. As shown in the figure 3.7 (a), four different microcapsules were produced. These capsules had unique colors since different food dyes were used for each microcapsule. The unique codes of microcapsules were generated using the patterned UV light. The codes were not observable under bright field microscopy. The fluorescent codes on the shells were clearly observed using a fluorescence illumination source and a filter. For example, the yellow microcapsules had circle array on the shells. The blue and green microcapsules showed fluorescent triangle and heart arrays, respectively. All types of colored microcapsules were collected in a vial and each fluorescent code was matched with each color. Various kinds of liquid inside the microcapsules can be identified by recognizing these codes on the microcapsules, which is necessary for generation of microcapsule library where all kinds of microcapsules are mixed in a bottle.

Also, as I use graphical codes, the total number of codes can be increased easily by our needs. For example, regarding character codes as shown in figure 3.7 (c),

I could use 60 kinds of codes for each spot of which the two spots are available on each particle. English has 52 alphabets including capital letters and the Arabic number has 10 letters. If I have two spots assigned for characters, I can have 3600 (= 60 x 60) codes (Figure 3.7). If I need more codes, I can use other country's alphabets or other special characters such as figure (e.g. polygon) and special characters (e.g. ‘?’, ’!’, ‘+’, ‘-‘, etc.).

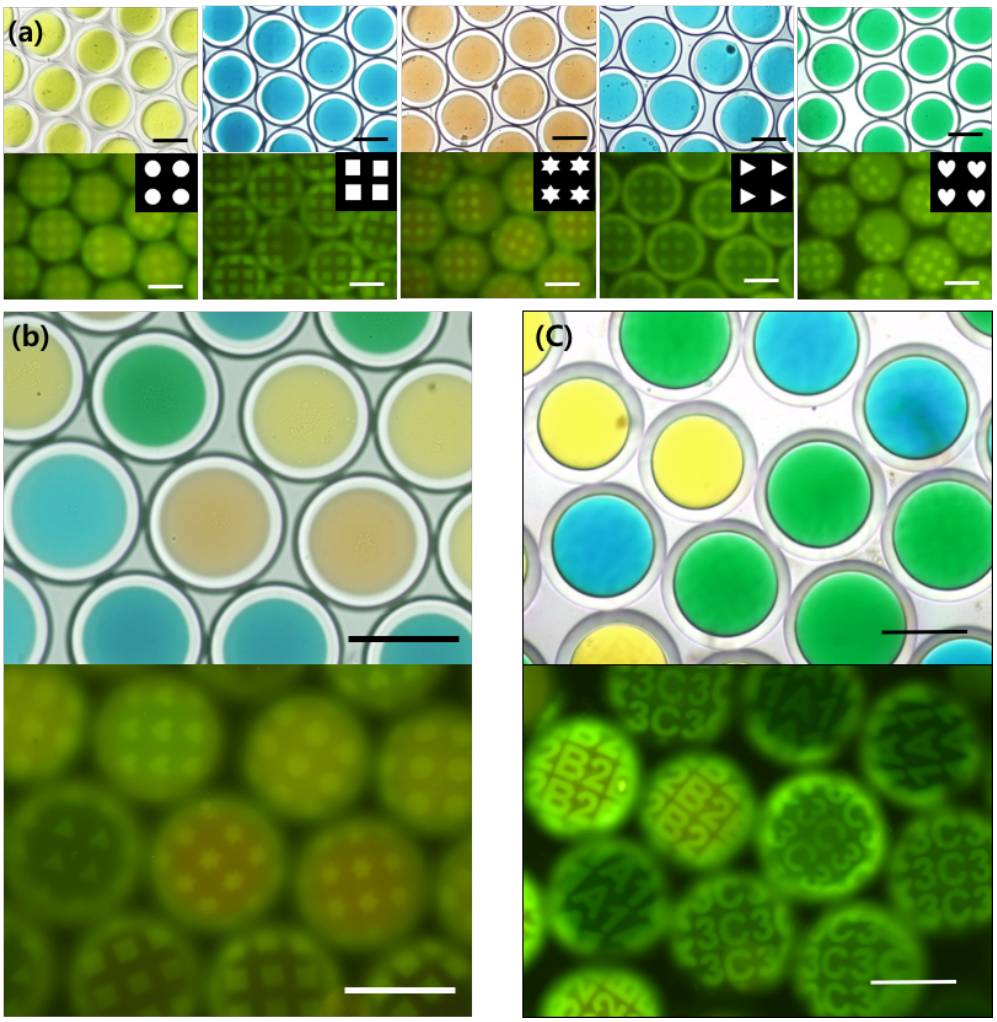

Figure 3.7 (a) Various compounds are encapsulated in the solid microcapsules and encoded to represent their contents. (b, c) Bright and fluorescence images of the microcapsules with shape code and character code. It shows that the fluorescently graphical codes exist on the shell of the microcapsule.

3.4 Characteristics of Code in Microcapsule

3.4.1 Variation of Fluorescence Intensity of encoded microcapsule

The fluorescent intensities of the code depend on the UV irradiation time and the initiator concentration in the PFPE. To measure the intensities according to the UV irradiation time, a microcapsule was exposed to UV light sequentially (wavelength: 365nm, 180mW/cm^2). As shown in figure 3.8, fluorescence intensity of the microcapsule increase according to total UV irradiation time until 600s exposure time.

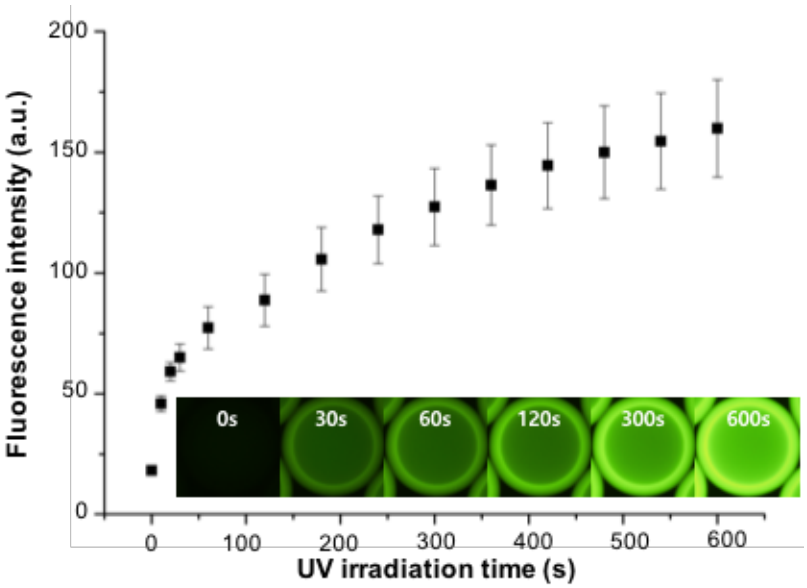

Figure 3.8 Variation in photoluminescence intensity among microcapsules, according to different UV irradiation times. The polymerized PFPE microcapsule is exposed to UV light sequentially. The fluorescence intensity of the microcapsule increase according to total UV irradiation time until 600s exposure time.

To measure effect of the initiator concentration in the PFPE, the PFPE solutions with three different concentrations of DMPA photoinitiator were prepared 1 wt%, 3 wt%, and 10 wt%, respectively. These solutions were poured onto glass slides and exposed to the patterned UV light for 30 seconds at 180 mW/cm^2. The fluorescent images were captured and the pixel color information was sampled. The intensity values were obtained and plotted on the graph. Given that the DMPA photoinitiator itself has photoluminescence under UV light, the intensity increased as the concentration of photoinitiator increased as shown in figure 3.9.

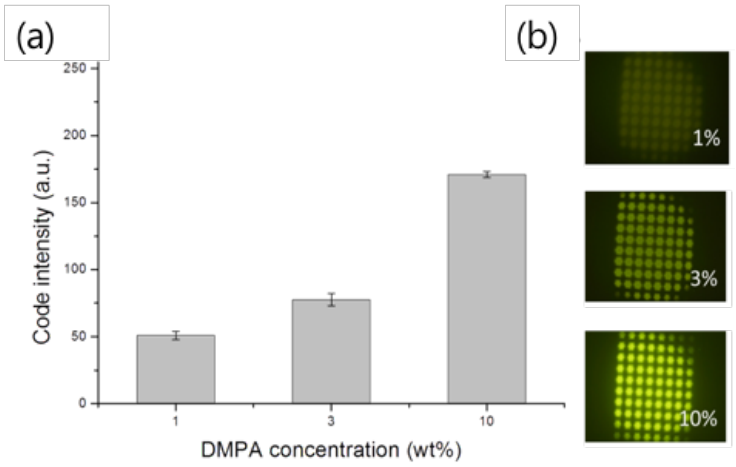

Figure 3.9 Fluorescent intensity variation with the different concentrations of DMPA photoinitiator. (a) Relationship between DMPA concentration and code intensity. (B) Images of code difference according to the variation of DMPA concentration. Given that the DMPA photoinitiator itself has photoluminescence under UV light, the intensity increased as the concentration of photoinitiator increased.

3.4.2 Code durability

To make encoded microcapsule library, the code of the microcapsule should maintain for a long time until they are used to assay. If the codes disappear as soon as they are generated, the different microcapsules with different biochemical contents cannot be distinguished from each other. To verify long time persistence of the code of microcapsule, microcapsules were prepared and encoded to test the durability of code. Firstly, microcapsules were dispensed in a 96-well plate and were stored in DI-water. The patterned UV light (365 nm, 180 mW/cm^2) was illuminated to the capsules through an objective lens using DMD device. Different characters on the shells indicate different UV irradiation times (character L: 10 seconds, N: 15 seconds, I: 20 seconds, B: 30 seconds). All cases exhibited long term code durability (Figure 3.10 (a)). No significant decrease in code intensity was observed in these cases. Thus, UV illumination needs at least 10 seconds at 180mW/cm^2 to generate codes. Among the encoded microcapsules, code character B was continuously monitored for 58 days and the intensity did not decrease significantly for 58 days (Figure 3.10 (b)).

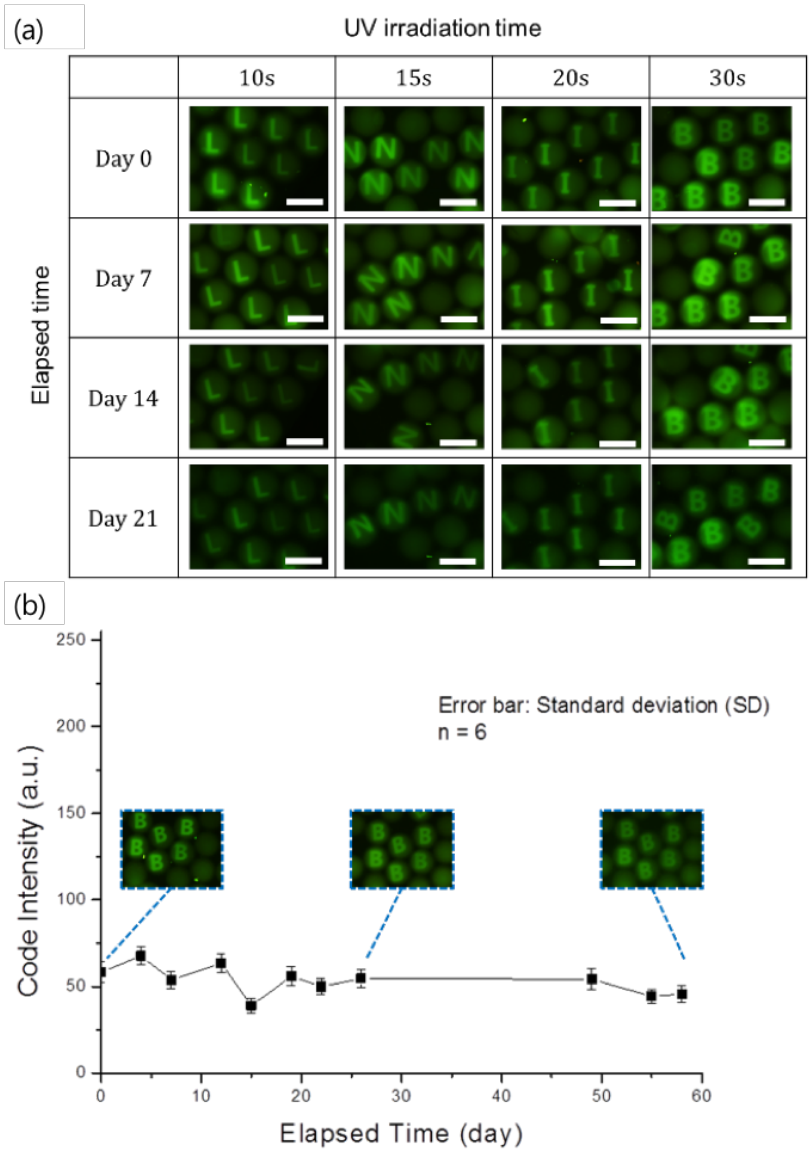

Figure 3.10 Code durability test. (a) Code durability with the different UV irradiation time. (b) The graph for the code intensity of "B" encoded microcapsules. The intensity of the code character B did not decrease significantly for 2 months.

3.5 Image Processing for Code Recognition

After assembly of the encoded microcapsules, images of whole microwell were obtained. Then, the code of each microcapsule in each position of the microwell are recognized and matched with its content inside (Figure 3.11), which will be used for analyzing multiplex assay results. To recognize code in microcapsule automatically, I programmed code recognition system with Matlab. First, in the microwell image, each microcapsule is recognized by circle recognizing algorithm based on the fluorescence difference (Figure 3.12 (a)). Each image of microcapsule is then processed by barcode or character code recognition program. In barcode and character code recognition, each image is rotated by Hough transform algorithm, cropped and stitched to obtain complete code image of the microcapsule. In barcode, by measuring thickness of each bar line, I can obtain correct code in microcapsule (Figure 3.12 (b)). In character code, align mark is added under the character to help rotation of image. By utilizing conventional optical character recognition (OCR) program, I can successfully recognize character code (Figure 3.12 (c)).

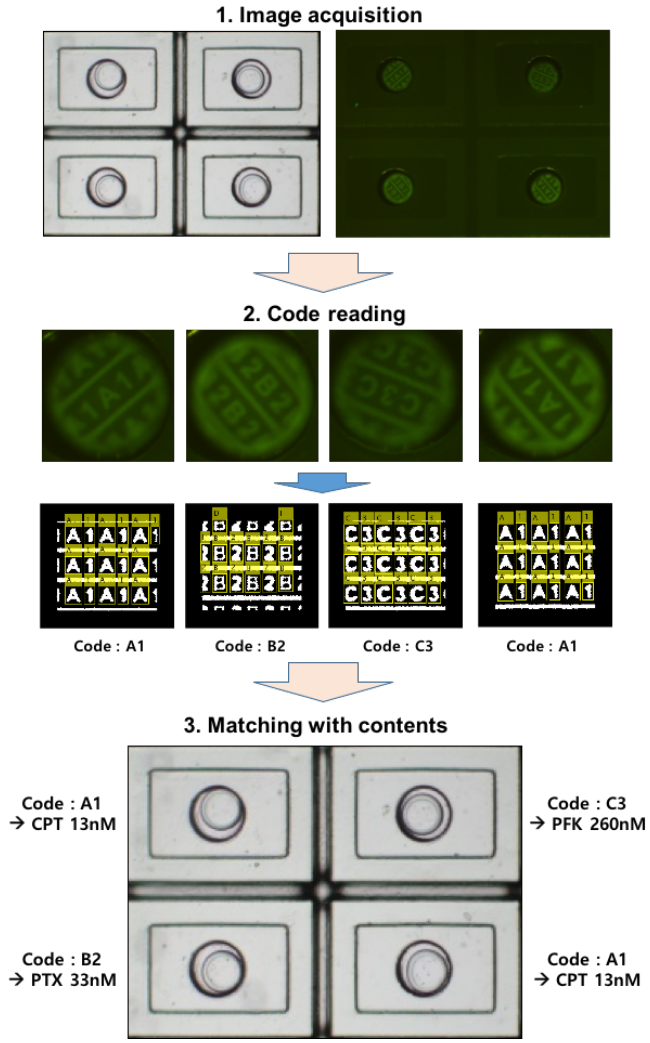

Figure 3.11 Whole process for matching microcapsules with their contents. After assembly of the encoded microcapsules, images of whole microwell were obtained. Then, the code of each microcapsule in each position of the microwell are recognized by code reading image process and matched with its content inside. After releasing and reaction process, the matched contents are used to analyze reactions in the microwells.

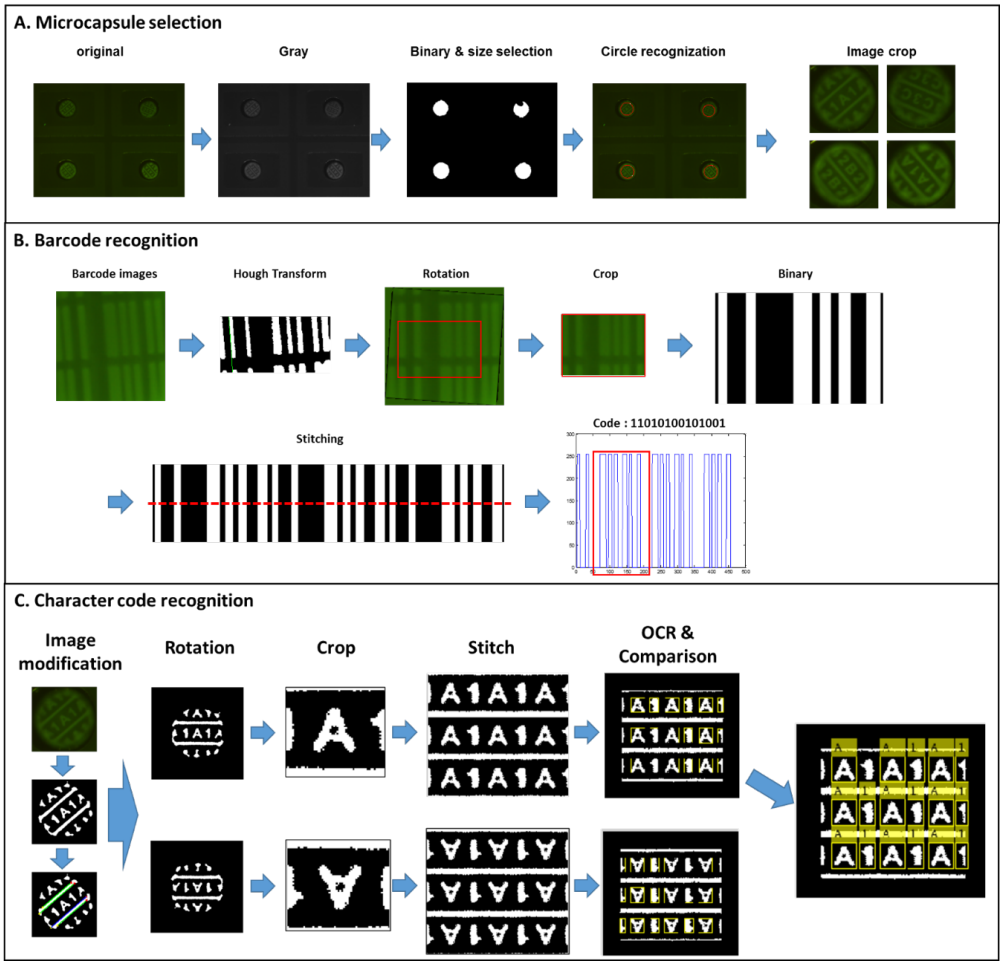

Figure 3.12 Image processing for code recognition. (A) In the microwell image, each microcapsule is recognized by circle recognizing algorithm based on the fluorescence difference. Each identified image of microcapsule is recognized by (B) barcode recognition process or (C) character code recognition process. In barcode and character code recognition, each image is rotated by Hough transform, cropped and stitched to obtain complete code image of the microcapsule. In barcode, by measuring thickness of each bar line, correct code in microcapsule can be obtained. In character code, align mark is added under the character to help rotation of image. By utilizing conventional optical character recognition (OCR) program, character code can be obtained.

Chapter 4

Platform Development for Multiplex assays

In this chapter, microwell array platform using the encoded microcapsule for multiplex assay applications is described. First, fabrication processes of the microwell and the micropillar array are described. Then, assembly process of the encoded microcapsule is also described. To estimate the code distribution of the encoded microcapsule after assembly, theoretical analysis with simulation of the binomial distribution is performed and compared with experimental result. To perform multiplex assay, liquid in each microcapsule should be released to react with reagent or cells in the microwell. I developed two type of liquid releasing methods, one is laser releasing system which utilize pulse-laser ablation, and the other is mechanical releasing system which utilize the micropillar array.

4.1 Fabrication of Microwell and Micropillar Array

PDMS microwell for laser releasing system was fabricated by conventional soft lithography technology. For the polyurethane acrylate (PUA) microwell generation for mechanical releasing system, a UV curable PUA monomer (MINS-311, Minuta Co., Korea) was poured on a PDMS master mold and an adhesion primer (Minuta Co., Korea) coated slide glass was placed on top of the uncured PUA monomer layer. After pushing the slide glass to make flat PUA surface, The PUA layer is exposed to UV (λ = 365 nm, 110mW/cm^2) for 60 seconds. The cured PUA microwell on the slide glass is detached from PDMS master mold and the detached PUA microwell is additionally cured for 60 seconds. Then, the slide glass is washed with ethanol to remove remaining adhesion primer on the surface of glass, which can be toxic to the cell.

In the case of micropillar array, flexible PET film (thickness = 100μm) was placed on top of the uncured PUA which was poured on the PDMS mold and exposed to the UV light. As the PET film has good bonding property with PUA material, it does not need to coat the surface of PET film with adhesion promoter. After UV curing, the cured micropillar array is peeled off from the PDMS master mold (Figure 4.1).

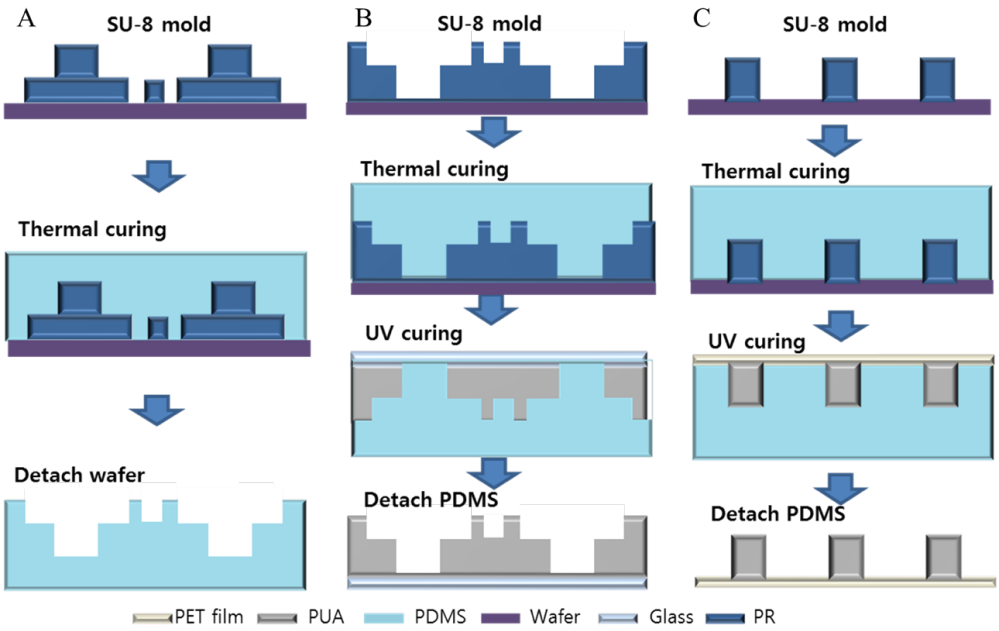

Figure 4.1 Fabrication process of microwell and micropillar array. (A) PDMS microwell fabrication. the PDMS microwell is fabricated by conventional soft lithography process. (B) PUA microwell generation process. The SU-8 microwell mold is double-casted with PUA monomer onto the adhesion promoter coated glass slide. (C) micropillar array generation. The SU-8 micropillar array mold is double-casted with PUA monomer onto the flexible PET film.

The microwell can consist of one or two layer. In the case of one layer microwell, height of the microwell (h1) should be higher than diameter of a microcapsule (d) and smaller than one and a half diameter of a microcapsule, which enables extra microcapsules to be removed easily by sweeping after assembly of microcapsules. In the case of two layer microwell, height of the first (bottom) layer is

same with the height of one layer microwell and height of the second layer should be smaller than a half of the diameter of a microcapsule for the same reason (Figure 4.2). Also, by changing design of the microwell, various combinations of the encoded microcapsules can be achieved.

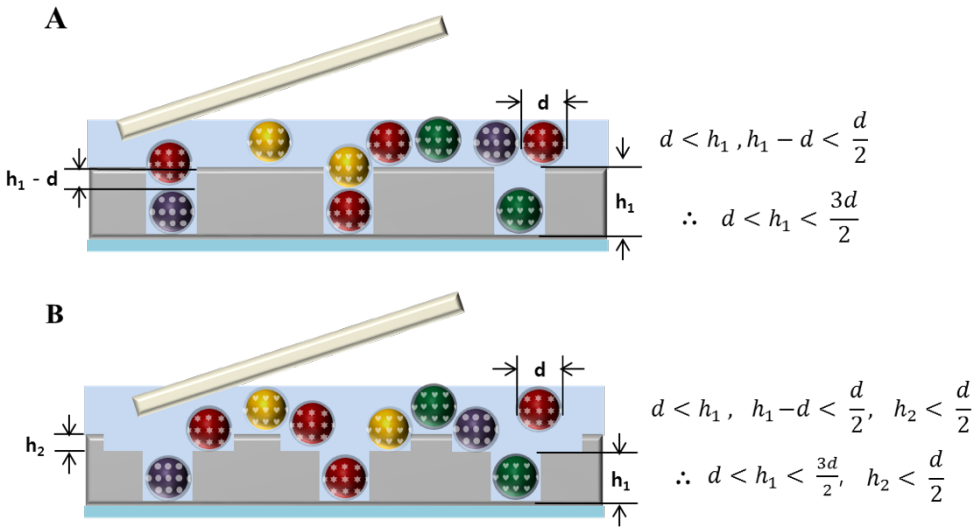

Figure 4.2 Designs of the microwell array. (A) Dimensions of one layer microwell. (B) Dimensions of two layer microwell. The height of the microwell is designed for one microcapsule to be assembled in one microwell and the other microcapsules can be easily removed.

4.2 Assembly of the Encoded Microcapsule

4.2.1 Self-assembly of the Encoded Microcapsule

For multiplex assay, encoded microcapsules in the pooled library are simultaneously self-assembled into the empty microwells in a single pipetting step, eliminating the labor-intensive serial dispensing process to aliquot liquids into the microwells. Heterogeneous microcapsules in the library are dispensed into the microwell array and swept by planar substrate such as slide glass or scrapper. By a few sweeping processes, microcapsules are assembled in almost every microwell. After assembly, extra microcapsules are easily removed from the microwell by additional sweeping processes. The spherical shape of the microcapsule facilitates assembly of the microcapsule in the microwell, enabling assembly efficiency to reach 99.5% (Figure 4.3). The self-assembly process of microcapsules takes only a few seconds, which is equivalent to thousands of serial dispensing steps requiring a few hours.

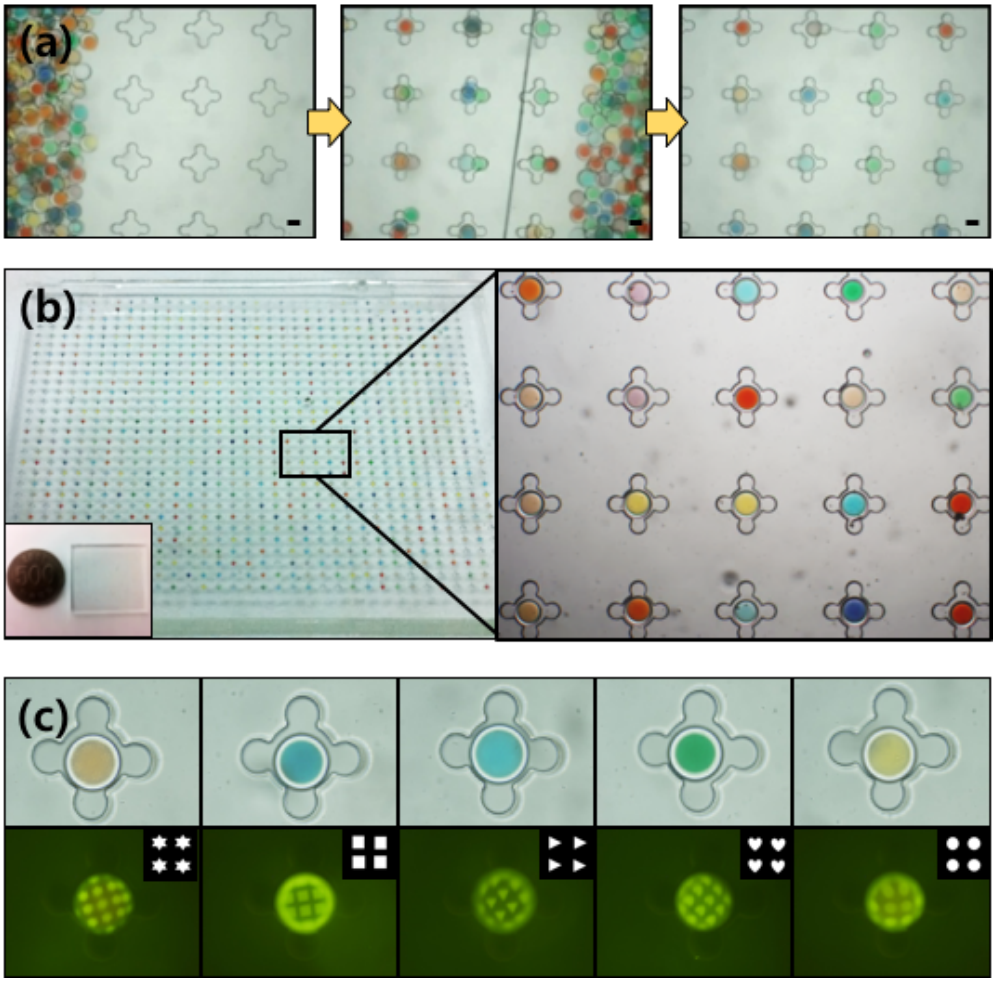

Figure 4.3 Self-assembly of the encoded microcapsule. (a) Process of the assembly. Encoded microcapsules are introduced within a single pipetting and self-assembled into the microwells by sweeping the microcapsules. After assembly, extra microcapsules are easily removed from the microwell by additional sweeping processes. (b) Images of the microwell array after assembly of the microcapsules. For visualization, various color dyes were mixed in the core liquid. The assembly efficiency of the microcapsules is 99.5%. (c) After assembly, each microcapsule assembled in each microwell can be identified by fluorescent graphical code of the microcapsule using fluorescence microscope.

Regarding to the combination of various compound, our platform has advantage in combinatorial assays, because assembly process occurs in a single pipetting process and independent to types of combinations of various compounds. As shown in figure 4.4 (a), various type of microwell can be fabricated by simply modifying design of the microwell. For example, in the four-leaf wells like figure 4.4 (b), right image, 715 ($=_{10+4-1}C_4$) and 40,920 ($=_{30+4-1}C_4$) combinations (calculated by combination with repetition) could be obtained with 10 and 30 different microcapsules, respectively with only single pipetting. Each combination also is identified by recognizing codes of the microcapsules.

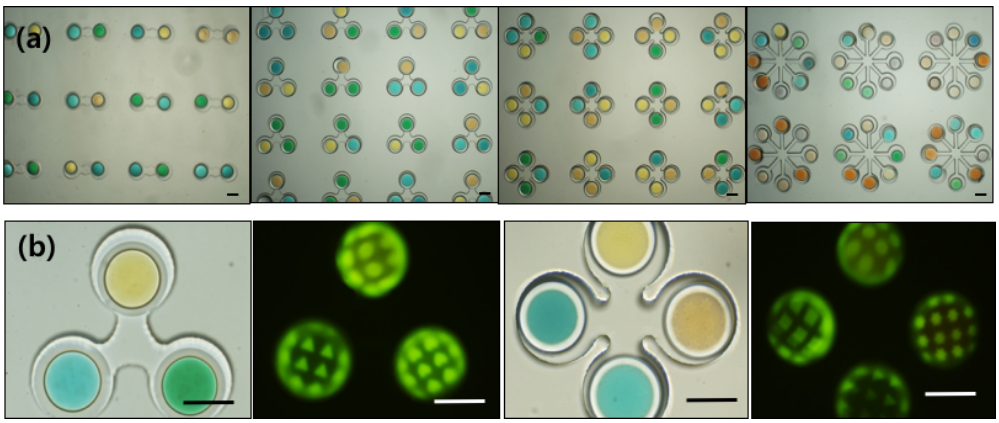

Figure 4.4 Combinatorial assembly of the differently encoded microcapsules. (a) Various designs of the microwell combinations. (b) The combination of liquids can be identified by decoding the code of the microcapsules in the microwell.

4.2.2 Binomial Distribution of the Encoded Microcapsule Assembled in the Microwells

As the assembly process of the encoded microcapsules follows the random distribution, the code distribution of microcapsules in the microwells should be verified for guaranteeing of the multiplex capability. To estimate the code distribution of the encoded microcapsules after assembly, I assumed that the assembly of the microcapsules with 10 different codes. When a microwell is filled with a microcapsule, the probability of a microcapsule with specific code is p = 1/10, while the probability of microcapsules with other codes is 1-p = 9/10. When I consider N microwells where the microcapsules are assembled, the probability of microcapsule with a specific code in k microwells follows a binomial distribution. A random variable X follows a binomial distribution with parameters n, k, and p, where, n is number of trials, k is number of successes, and p is probability in each trial. The probability mass function of X follows equation.

$$f(k;n,p) = \Pr(X = k) = \binom{n}{k} p^k (1-p)^{n-k}$$

Figure 4.5. show that the probability density function of binomial distribution for the assembly of the encoded microcapsule with a specific code. Here, I assumed that the microcapsules have 10 different codes and are assembled in 100 microwells. When I consider minimum value of the number of assembled microcapsule from our experiment, the probability that more than 4 microcapsules with a certain code are

assembled in the microwell is about 99.22%.

$$\Pr(4 \leq X) = 0.9922$$

Theoretically, the average number of microcapsules with a certain code in 100 microwells is E(X) = np = 10. If I increase the number of the microwells, all drug candidates can be covered at one experiment with high probability.

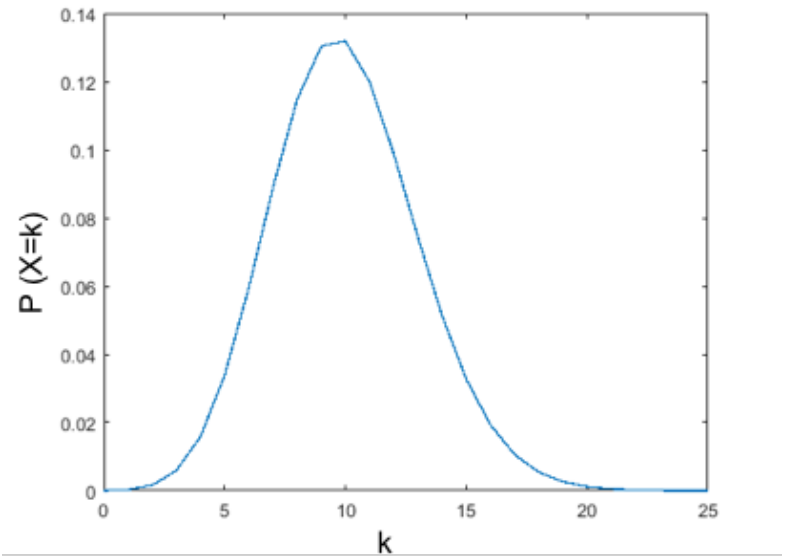

Figure 4.5 Probability density function (X=k) generated by a binomial distribution for the assembly of the encoded microcapsule with a specific code. Assumed that microcapsules with 10 different codes are assembled in 100 microwells.

In experiment, I assembled the encoded microcapsules with 10 different codes and counted codes of the microcapsules in every 100 microwells. As shown in figure 4.6, I observed that average number of assembled microcapsules per each code

in the microwell is nearly 10, which are matched with theoretical mean of the binomial distribution

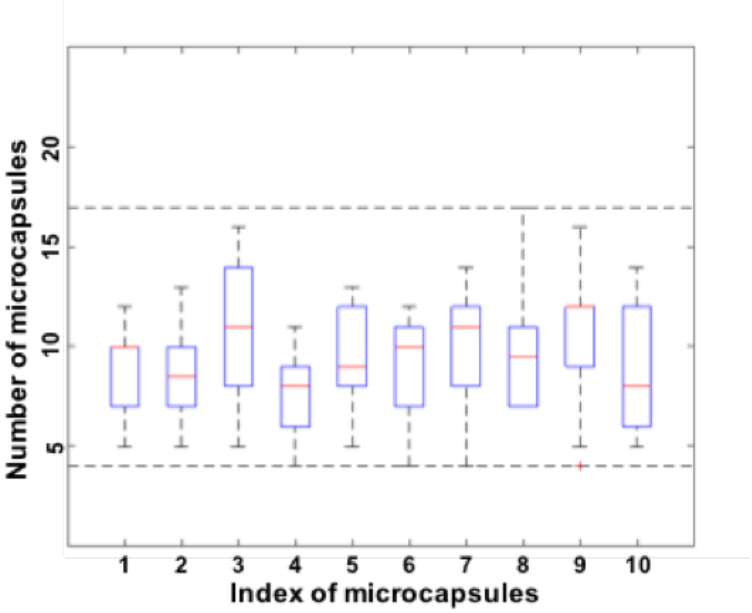

Figure 4.6 Distribution of the 10-differently encoded microcapsules assembled in the microwells. On average, about 10 microcapsules of each code were assembled in a hundred microwells.

4.2.3 Transfer of the microcapsule array

As a different approach, I developed method for transferring microcapsule array to the other substrate, generating embossed microcapsule array. After assembly of the microcapsules in the PDMS microwell array, photo-curable solution such as

PFPE or PEG-DA is coated on the top surface of the microwell array. Then, solid substrate is laid on the PFPE or PEG-DA solution. The coated PFPE or PEG-DA solution is then polymerized by UV irradiation. After UV exposure, polymerized PFPE or PEG-DA coating layer with solid substrate is detached from the microwell array. Because of inhibition layer of PDMS, polymerized PFPE or PEG-DA layer can be easily detached from the microwell. The microcapsules are attached to cured PFPE or PEG-DA layer, generating embossed microcapsule array on the solid substrate (Figure 4.7 (a)). When I used PFPE as a coating layer, because of high viscosity of the PFPE solution, the PFPE solution does not penetrate into the microwell but only contact with the assembled microcapsules in the microwells, making the microcapsules to be laid on the PFPE layer as shown in figure 4.7 (b). In the case of PEG-DA, because of low viscosity of the PEG-DA than the PFPE, the PEG-DA solution penetrates into the microwell making the microcapsules to be fully covered with PEG-DA layer as shown in figure 4.7 (c).

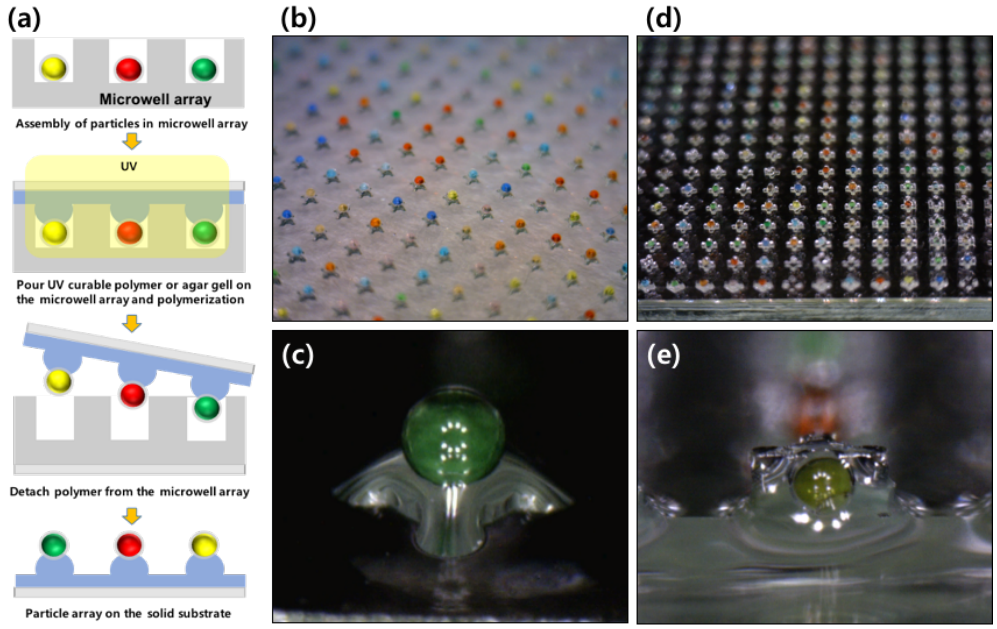

Figure 4.7 Transfer of the microcapsule array. (a) After assembly of the microcapsules in the PDMS microwell array, photo-curable solution is coated on the top surface of the microwell array. Then, solid substrate is laid on the solution. The coated solution is then polymerized by UV irradiation. After UV exposure, polymerized coating layer with solid substrate is detached from the microwell array. The microcapsules are attached to cured layer, generating embossed microcapsule array on the solid substrate. Microcapsule array has different feature according to the coating materials such as (b, c) PFPE and (d, e) PEG-DA

4.3 Releasing of the Liquid inside the Microcapsule

With our platform, a multiplex assay can be conducted by reacting a single target sample in the microwell and various liquid reagents in the microcapsules. The various regents are separated in the microcapsules as well as the target sample along with the microcapsule in the microwell. The microwells are isolated from each other by covering them with immiscible oil. Next, each reagent in the microcapsule is released to react with the target sample in the isolated microwell. Releasing systems are developed using two different methods. One is a laser releasing system, and the other is a mechanical releasing system.

In the laser releasing system, I employed nanosecond pulse laser equipment for laser induced rupture of the microcapsule. By applying a pulse laser to a desired location of the microcapsule in the PDMS microwell, I selectively or sequentially released the core liquid into the microwell. However, to rupture the microcapsule, laser light should be specifically focused on the shell of each microcapsule, which is difficult and laborious. Additionally, heat or shock waves generated after laser illumination may denature the reagent or alter the reagent properties in the microwell.

To resolve these problems, I also developed a mechanical releasing system. I constructed a micropillar array on the flexible PET film where the each micropillar fit into the each microwell. Here, I used PUA as the microwell material and the micropillar array because of its high rigidity. By pushing and sweeping the micropillar

array aligned with the microwell array, the microcapsule is directly pressed and broken by the micropillar, and then the core liquid is released into the microwell. Using a motorized stage and pressing equipment, whole microcapsules in the microwells can be broken automatically within a few minutes. Using this method, both the release accuracy and throughput are enhanced without damage to the reagents or samples.

4.3.1 Laser Releasing System

For reaction of our platform, the core liquid should be released from the shell of the microcapsule and be reacted with surrounding liquid in the microwell. Here, I developed pulse laser equipment utilizing laser induced ablation of microcapsule (Figure 4.8). The equipment consists of motorized moving stage, CCD camera and nanosecond pulse laser (MiniliteNd:YAG laser, Continuum Inc., maximum power: 12mJ at 532nm, pulse duration: 7ns). The microcapsules are assembled in the microwell and the microwell is sealed with slide glass to prevent evaporation of surrounding liquid in the microwell and placed on the motorized stage. By applying on laser pulse, the shell of the microcapsule is broken by laser ablation and core liquid inside the microcapsule is released to the microwell and mixed with surrounding liquid (Figure 4.8 (c)). This laser breakage system enables selective and sequential releasing of core liquid in the microwell array.

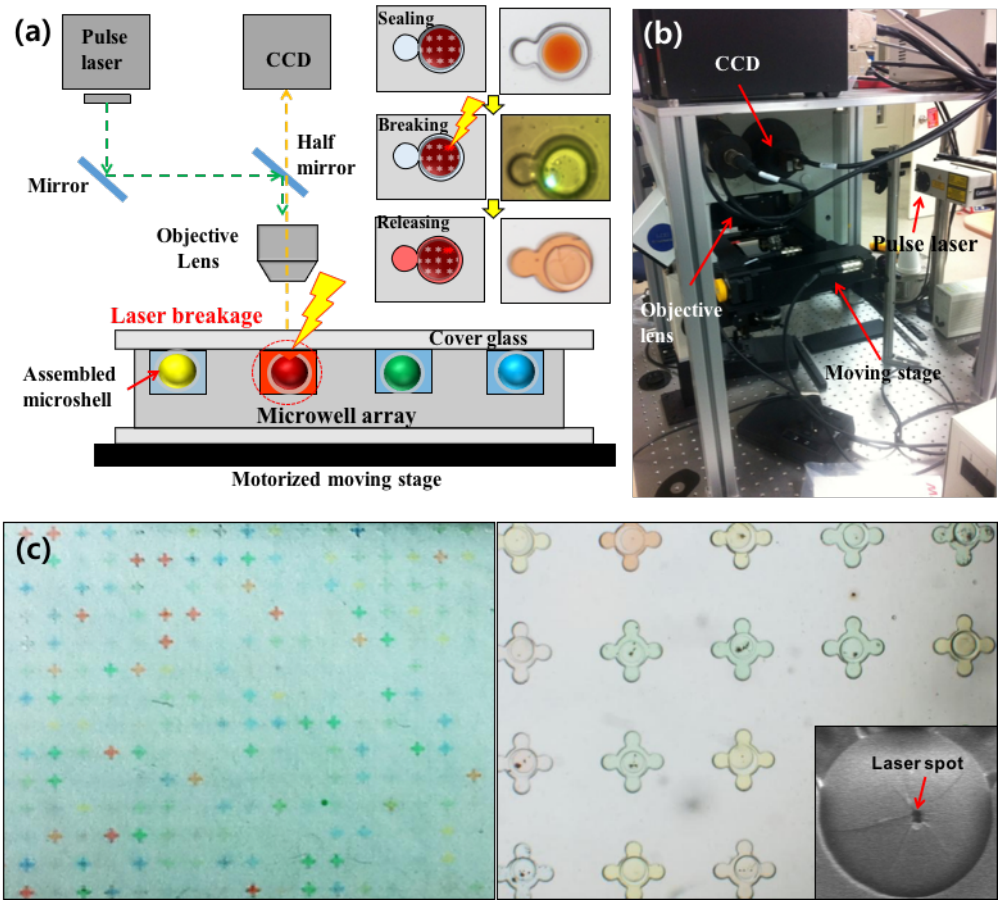

Figure 4.8 Pulse laser releasing system. (A) Schematic image of pulse laser releasing process. After assembly of microcapsules, microwell array is sealed by slide glass to isolate each well and prevent evaporation of surrounding medium. When the pulse laser is focused and applied on shell of the microcapsule, the shell is broken by laser ablation and core liquid of microcapsule is released and diluted with surrounding liquid of microwell. (B) Experimental setup of pulse laser releasing system. The setup consists of Nd:YAG pulse laser, CCD and motorized moving stage. (c) Releasing results of the microcapsules using pulse laser system. Inset is SEM image showing broken microcapsule by pulse laser.

4.3.2 Mechanical Releasing System

In the case of the laser releasing system, the laser light should be specifically focused on the shell of each microcapsule to rupture the shell of the microcapsule, which is difficult and laborious. Additionally, heat or shock waves generated after laser illumination may denature the reagent or alter the reagent properties in the microwell. To resolve these problems, I also developed a mechanical releasing system utilizing a micropillar array that can be aligned with the microwell array. I fabricated a micropillar array on the flexible PET film where each micropillar fit into each microwell. The PDMS microwell is too elastic to transfer mechanical force to the microcapsule entirely and thereby hinders breakage of the microcapsule. So, I used PUA as a material of the microwell and the micropillar array because of its high rigidity. The PUA microwell where the microcapsules are assembled is covered with the immiscible silicone oil to prevent reagents evaporation and cross-contamination between microwells. The oil phase also prevents overflow of the inner liquid in the microwell during breaking of the microcapsule by the micropillar. The micropillar array is then aligned with the microwell array and smoothly pushed and swept with to break the shell of the microcapsule in the microwell. After breakage process, various types of the core liquids in the microcapsules are released into the individual microwells and react with reagents filled in the microwells.

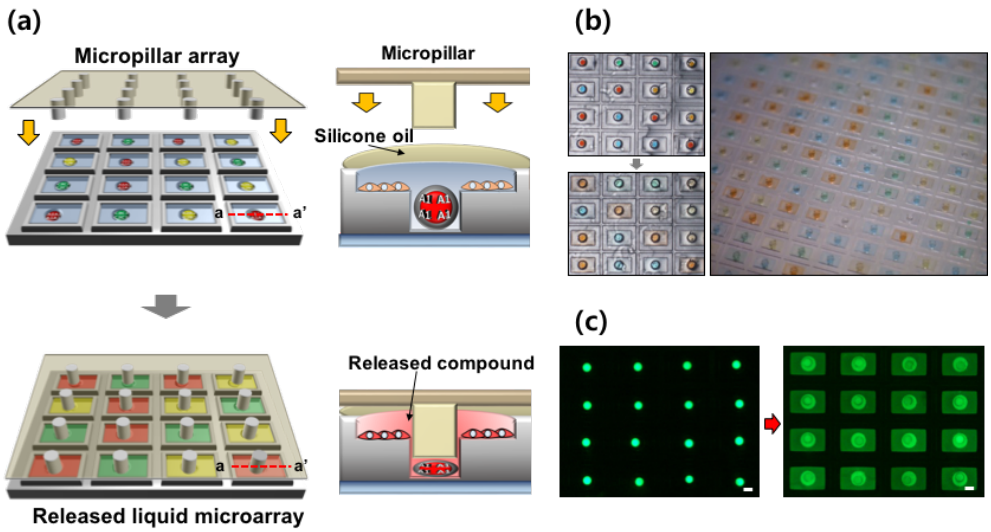

Figure 4.9 Mechanical releasing system. (a) Schematic images of mechanical releasing system. After assembly of microcapsules, the microwell array is sealed with immiscible oil to prevent evaporation and cross contamination. The micropillar array fabricated on flexible PET film is then aligned with the microwell array. By pushing the micropillar array, the microcapsules are burst and the core liquid is released. (b) Images of the microwell array before and after releasing. The colored core liquid is released and diluted with liquid in the microwell. (c) Image of the microwell using fluorescence dye containing microcapsule. The results show that the liquid inside the microwell is well isolated and has no cross-contamination to other microwell.

For automation of mechanical releasing method, I employed motorized stage and ball bearing equipment (Figure 4.10). The equipment consists of microscope, motorized stage, ball bearing and x-y stage for ball bearing structure. The x-y stage is

fixed in body of the microscope and independent to movement of motorized stage. The microwell and micropillar array is aligned on the motorized stage and the ball bearing equipment is aligned at the microwell to be scanned. After pushing and fixing z-axis of the ball bearing on the micropillar array substrate, the motorized stage moves toward designed route to scan whole microwells. As the micropillar which is forced by ball bearing squeeze each microcapsule, the microcapsule is ruptured and core liquid is released. Using a motorized stage and pressing equipment, whole microcapsules in the microwells can be broken automatically within a few minutes. Using this method, both the release accuracy and throughput are enhanced without damage to the reagents or samples.

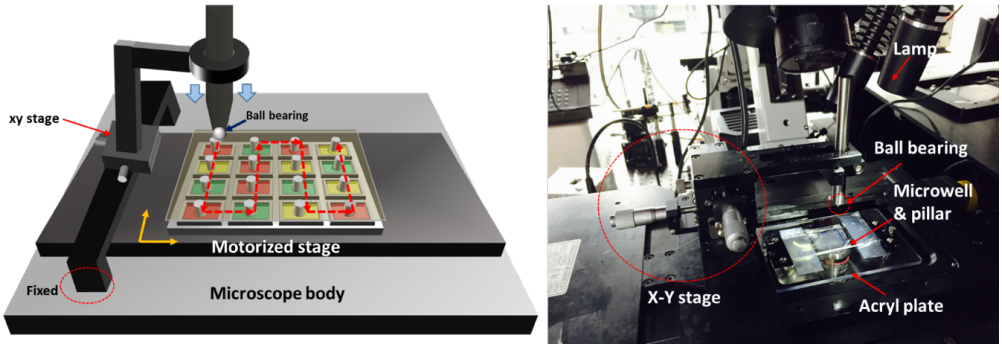

Figure 4.10 Automated mechanical releasing equipment. The equipment consists of motorized stage on the microscope, ball bearing and x-y stage to control location of ball bearing.

Chapter 5

Applications of the Encoded Microcapsule for Multiplex Assays

In this chapter, to validate that our platform can be used for various liquid-liquid or liquid-cell reactions, I performed enzyme inhibitor screening with β-galactosidase, virus transduction and a drug-induced apoptosis test using osteosarcoma cells (U2OS) and anticancer drugs. The results including the dose-response curves and the corresponding IC50 values of enzyme inhibitor screening and cell viabilities of drug-induced apoptosis test are compared with the results obtained using a conventional well-plate platform, to confirming that the encoded microcapsule can be an efficient alternative liquid-format screening platform.

5.1 Evaporation Test of the Microwell

For liquid-liquid reaction or liquid-cell reaction, it is important issue to control humidity for prevention of evaporation inside the microwell during incubation. For example, in cell-based assays, the cells need to be incubated for a few days to analyze results such as protein expression and drug induced cell death. So, I developed humidity chamber. The chamber consists of two space, one is for supplying humidity and the other is for incubation of the microwell. To supply humidity, the space consists water and tissue. The tissue is for increasing of wet surface, which increase evaporation in the space. In incubation chamber, the microwell is laid on the water-containing dish to increase humidity of the space. The microwell is then sealed with immiscible silicone oil to prevent evaporation of the microwell. Figure 5.1 shows results of evaporation test. Blue food dye is used to check degree of the evaporation. Liquid inside the microwell sustain 72 hours without evaporation. After 96 hours, evaporation occurs in some microwells. To improve prevention of evaporation, slide glass can be covered on the microwell.

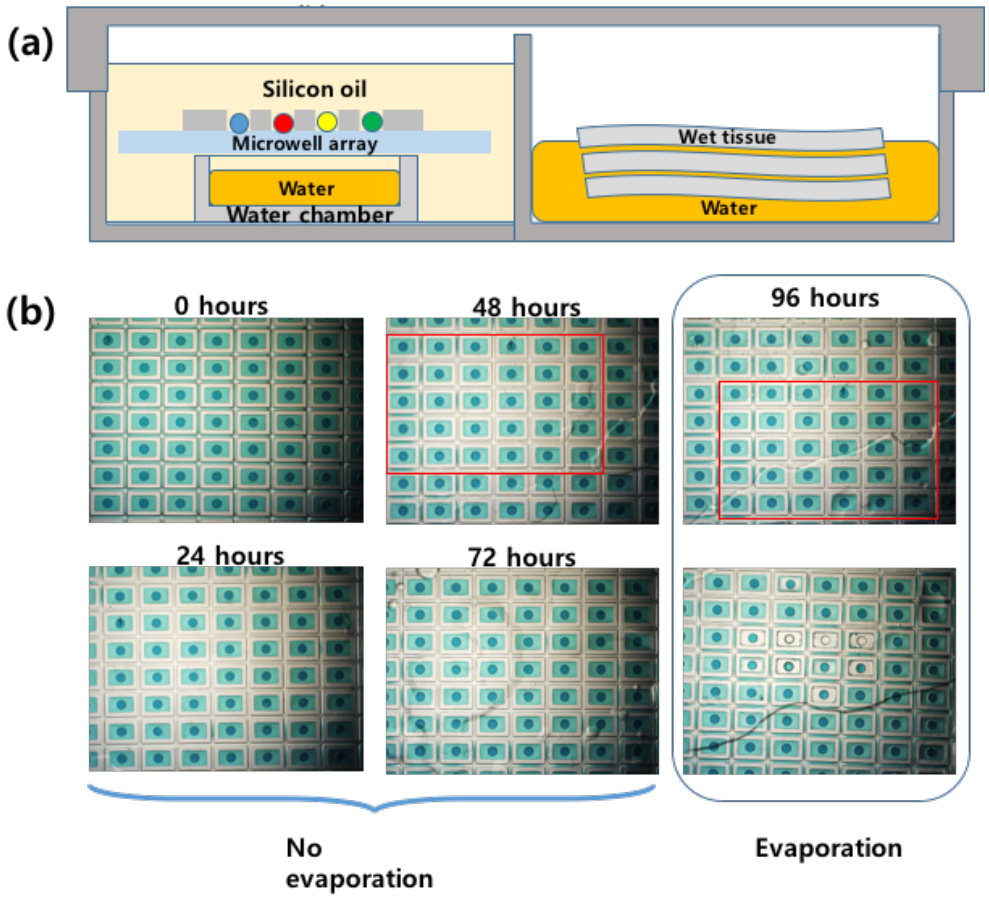

Figure 5.1 Evaporation test of the microwell. (a) The incubation chamber consists of two space, one is for supplying humidity and the other is for incubation of the microwell. Water in supplying chamber and bottom of the microwell supply humidity of the microwell and prevent evaporation of the microwell. (b) Evaporation test results. Blue food dye is used to check degree of the evaporation. Liquid inside the microwell sustain 72 hours without evaporation. After 96 hours, evaporation occurs in some microwells. Red rectangle indicates same area of the microwell.

5.2 Enzyme Inhibitor Screening

To validate that our platform is applicable to various library-screening approaches, I first conducted enzyme inhibitor screening. Here, I utilized β-galactosidase (β-gal) enzyme as a target sample and its known inhibitor, 2-phenylethyl β-D-thiogalactoside (PETG), a liquid reagent. For visualization, I utilized the fluorogenic substrate, fluorescein di-β-D-galactopyranoside (FDG), which is converted into fluorescent fluorescein by β-gal.

The microcapsule library was prepared by encapsulating a mixture of various concentrations of PETG and a constant concentration of FDG in the microcapsules. As the volume of the core liquid is 4.2 nL and the total volume of the microwell considering the volume of the microcapsule is 62.6 nL, the core liquid is diluted to 1/15 after releasing in the microwell. Thus, I set the concentration of core liquid in the microcapsule 15 times higher than the desired concentration of the microwell after the release. The stock solution of the microcapsule library was exchanged with β-gal solution so that the target enzyme and microcapsules were floated together and loaded into the microwell at the same time. After loading, the microwells were covered with immiscible oil to prevent cross-contamination between the microwells. Next, PETG and FDG in the microcapsules were released by breaking the microcapsule using the micropillar array. PETG released from the microcapsule inhibited the activity of β-gal, which converts FDG into galactose and fluorescent fluorescein molecule. As a result,

the each microwell produced different fluorescence intensities according to the concentration of PETG in each microcapsule (Figure 5.2 (a)). I obtained the time-course profile of fluorescence intensity at each inhibitor concentration (Figure 5.2(b)). The dose-response curves and corresponding IC50 values obtained using our platform showed good agreement with the results obtained using conventional well plate platforms (Figure 5.2 (c)).

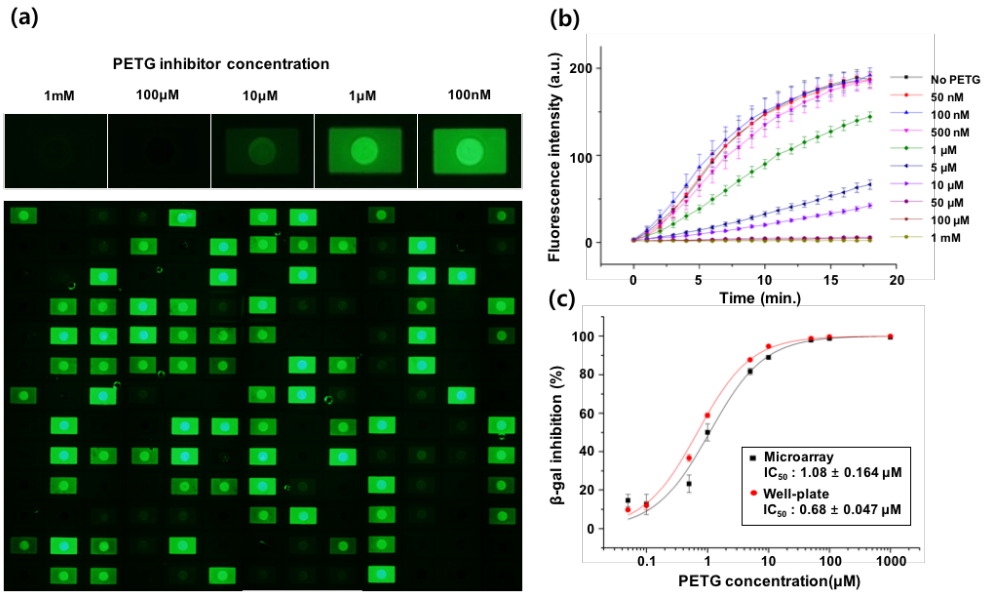

Figure 5.2 Enzyme-inhibitor screening results. (a) The enzyme (β-galactosidase) inhibitor screening results obtained after releasing the inhibitor (PETG) and substrate (FDG). (b) Time-lapse profile of enzymatic kinetic. (c) Dose-response curves of the PETG inhibitor obtained by the encoded microcapsule and the conventional well plate platform.

5.3 Virus Transduction

The platform also can be applied to cell-based assays. I performed virus transduction testing by using U2OS human osteosarcoma cells. After seeding and attachment of a single type of cells in the microwells, microcapsules containing various virus or drugs solutions were assembled into the microwells and the microwell was covered with a thin layer of immiscible and gas-permeable silicone oil. This oil layer prevented the evaporation of cell culture medium and successfully isolated the cell-seeded reaction chambers while enabling cells to survive during incubation. The microcapsules were then broken using the micropillar array and the viruses in the core liquid were released and penetrate the cells. After releasing of the viruses, the microwells were incubated under humid conditions and then gently immersed into PBS to wash and remove silicone oil on the microwells.

For virus transduction, the microwell was further incubated in fresh culture medium after PBS washing, giving cells sufficient time to express proteins after virus transduction. Figure 5.3 shows the virus transduction results of U2OS cells in the microwell array with adenovirus containing genes for red fluorescent protein (ad-RFP) and green fluorescent protein (ad-GFP). This result showed that our platform could be used for the analysis of various gene functions in cell microarrays.

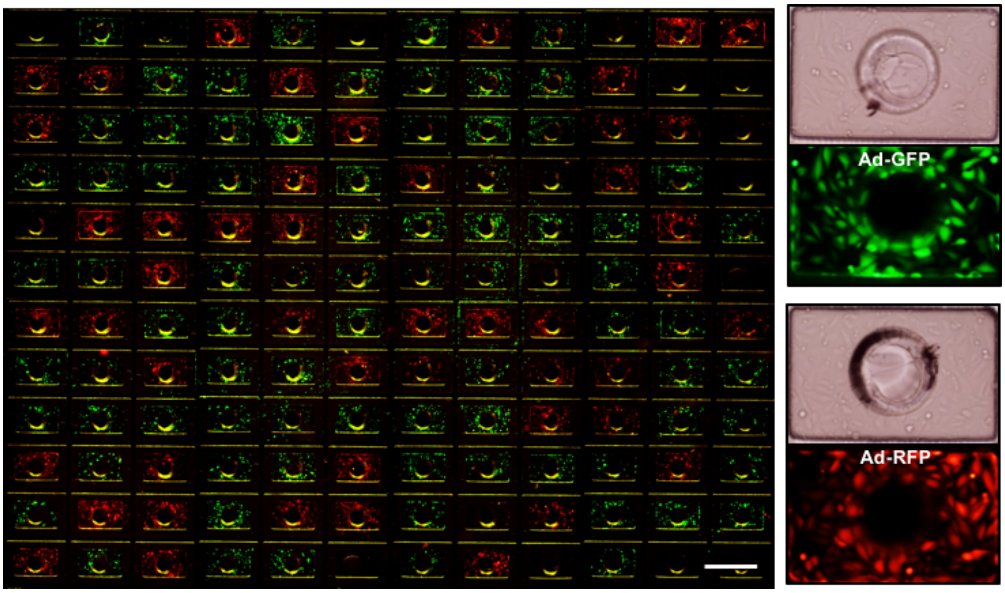

Figure 5.3 Viral transduction experiment. Microcapsules encapsulate adenoviruses containing genes for red fluorescent protein (RFP) or green fluorescent protein (GFP). The microcapsules are assembled in U2OS cell-seeded microwell and the core liquid is released. The adenoviruses in the released core liquid then penetrate into the cells and the GFP or RFP gene in adenovirus is delivered to U2OS cells in each microwell. After incubation, the GFP or RFP gene in the U2OS cell is expressed and red or green fluorescence can be detected in each microwell.

5.4 Drug-induced Apoptosis Test

In the drug-induced apoptosis test, I tested three different anticancer drugs at 4 different concentrations: camptothecin (CPT, 200 nM–200 μM), PKF118-310 (PKF, 40 nM–40 μM), and paclitaxel (PTX, 50 nM–50 μM). U2OS human osteosarcoma cells were cultured in McCoy's 5A culture medium with 1% of penicillin-streptomycin and 10% of Fetal Bovine Serum at 37°C under 5% CO2 incubation chamber. Cultured cells were detached from culture flasks using 0.25% trypsin and 0.13% EDPT in phosphate buffered saline (PBS). The centrifuged cells were dispersed in a cell culture medium prior to seed. The PUA microwell array was sterilized in an autoclave for 20min under 120°C, followed by oxygen plasma for 1 min. Then the PUA microwell array was treated with 5μg/mL fibronectin solution in PBS, incubated for 1h and then washed with PBS three times. Cells were seeded in PUA microwell array and allowed to settle down into the microwell array for 30 min. The seeding density of cells was adjusted to set a cell density of approximately $4x10^5$ cells/mL, resulting in about 200 cells per well. After cell seeding, cells in the microwell array were cultured in incubation chamber for 12h prior to use.

Figure 5.4 shows the process of drug-induced apoptosis test. The drugs at various concentrations were encapsulated in microcapsules, assembled, and released into cell-seeded microwells. Before assembly, stock solution of the microcapsules containing anticancer drug were exchanged with serum free medium prior to use and

the PUA microwell array is immersed in serum free medium. Microcapsules were assembled into the microwell array by sweeping several times and the microwell was sealed with silicone oil. The PUA microwell array was then aligned with the PUA micropillar array and microcapsules were broken by mechanical force and core drugs were released into the each microwell. After releasing of drug, the PUA microwell array was incubated for 12h to allow reaction between drugs and cells. After reaction with the drugs, the PUA microwell array was gently immersed into PBS to wash and remove silicone oil which covered chip and stained with apoptosis detection solution (FITC annexin V apoptosis detection kit, BD PharmingenTM) and membrane permeable DNA staining dye (Hoechst 33422, Invitrogen) for 1h in an incubator.

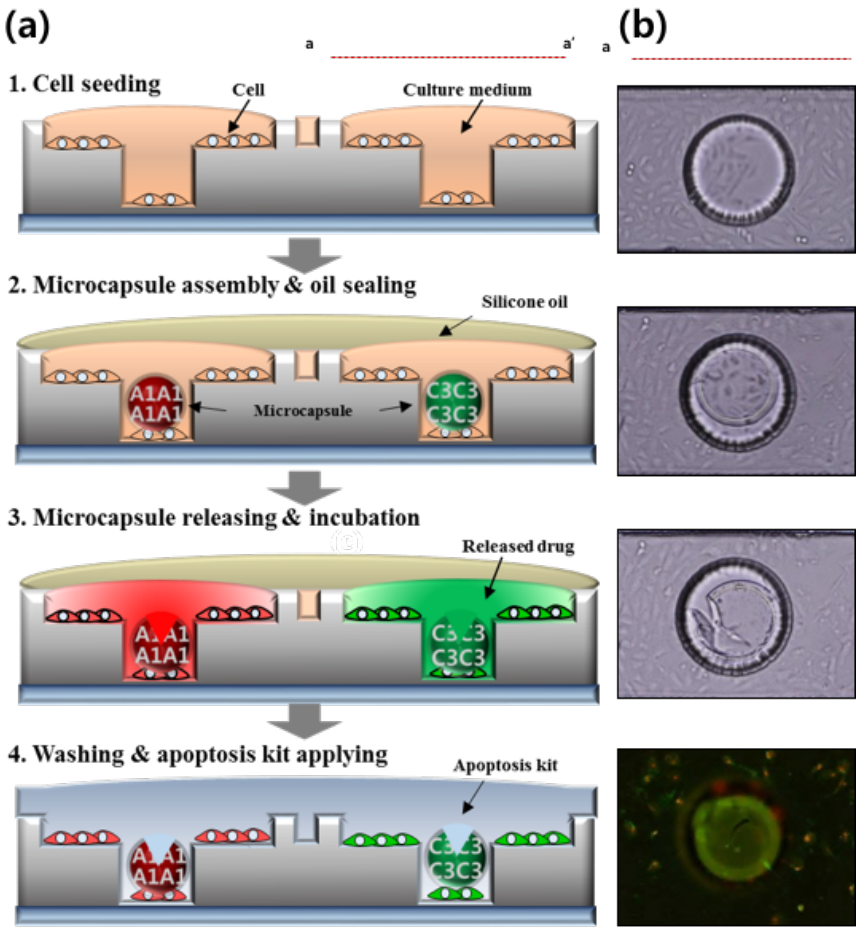

Figure 5.4 (a) Process of drug-induced apoptosis test. Cancer cells are seeded in the microwell and incubated to attach cells on substrate of the microwell. The microcapsules which containing anticancer drugs are assembled in the microwells, and the microwells is sealed with silicone oil to prevent evaporation and cross-contamination. The microcapsules are then broken and the core drug is released and react with cells in the microwell. After a few days incubation, the microwell is washed with PBS and apoptosis detection kit is applied to cells. (b) Images of cells in the microwell according to process of drug-induced apoptosis test.

The number of stained cells was counted by analyzing the fluorescent images, and cell viabilities were determined for the various drug concentrations via image processing. The cell viabilities obtained using our platform were compared to those obtained using a conventional 96-well plate platform to demonstrate the reliability of our platform as shown in figure 5.5. Blue bars represent the cell viabilities obtained using a conventional well plate platform as reference data, and red bars represent the cell viabilities obtained using our platform. The results for viability in our platform were comparable to those obtained using a well plate platform, demonstrating the feasibility of our platform for cell-based assays. The main advantage of using the microwell is that I can reduce the consumption of reagent, cells, and viruses. This advantage has more impact especially when the amount of rare sample (e.g. rare cells or viruses) are insufficient for the conventional wellplate based experiments.

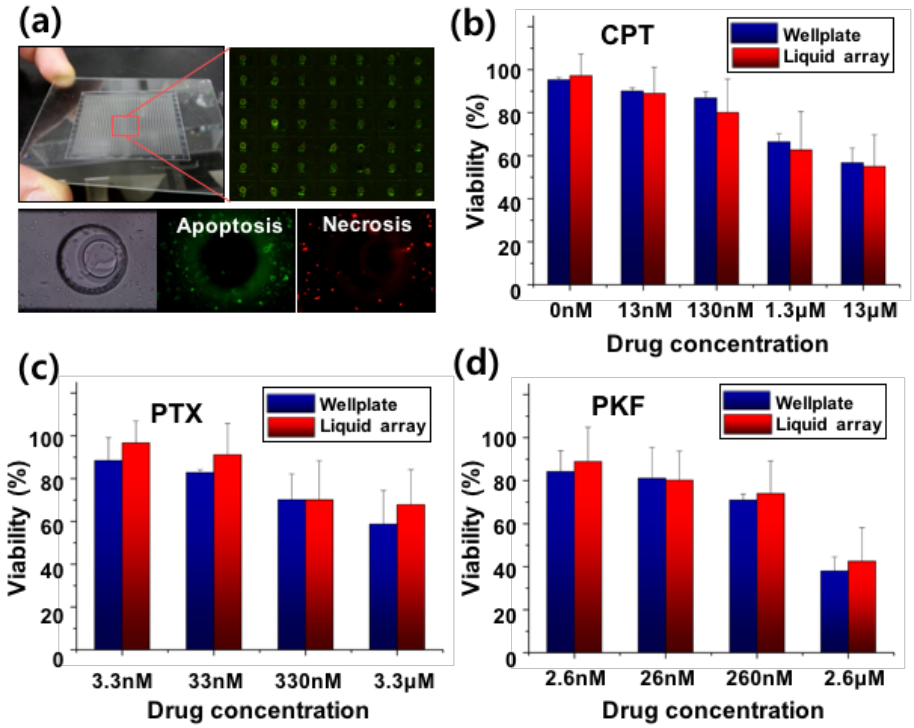

Figure 5.5 Drug-induced apoptosis test results. (a) Images of the microwell after drug-induced apoptosis test. The drug-induced apoptosis test was performed for three anticancer drugs at various concentrations: (a) camptothecin, (CPT, 0 nM: control, 200nM–200μM), (b) PKF118-310 (PKF, 40 nM–40 μM), and (c)paclitaxel (PTX, 50 nM–50 μM). Cells showing apoptosis and necrosis are labeled with green and red fluorescence, respectively. Blue bars represent results from the conventional well plate-based assays and red bars represent results from the microwell-based assays.

5.5 Image Processing for Apoptotic Cell Counting

To analyze drug-induced apoptosis results in conventional 96-well plate and our microwell array, I adopted CellC algorithm to count apoptosis cells through fluorescent images[69]. In the results of 96-well plate, fluorescent images of apoptotic cells in each well are directly analyzed with the algorithm. In the results of the microwell array, I first obtained fluorescent images of the microwell array in 4X microscope objective view (Figure 5.6). Each 4X image is cropped to obtain region of interest (Figure 5.6 (a, b), red rectangle) to have one microwell per on image. Each image is modified to remove any fluorescence noise coming from microcapsules, which can interrupt counting of apoptotic and total cells. Here, I replaced the area where the microcapsules are assembled with background color of the microwell. (Figure 5.6 (a, b), orange circle). After that, all microwells were analyzed by cell counting software to count the number of apoptotic cells and total cells (Figure 5.6 (c)). The viability was then calculated by dividing the number of apoptosis cells with total cells.

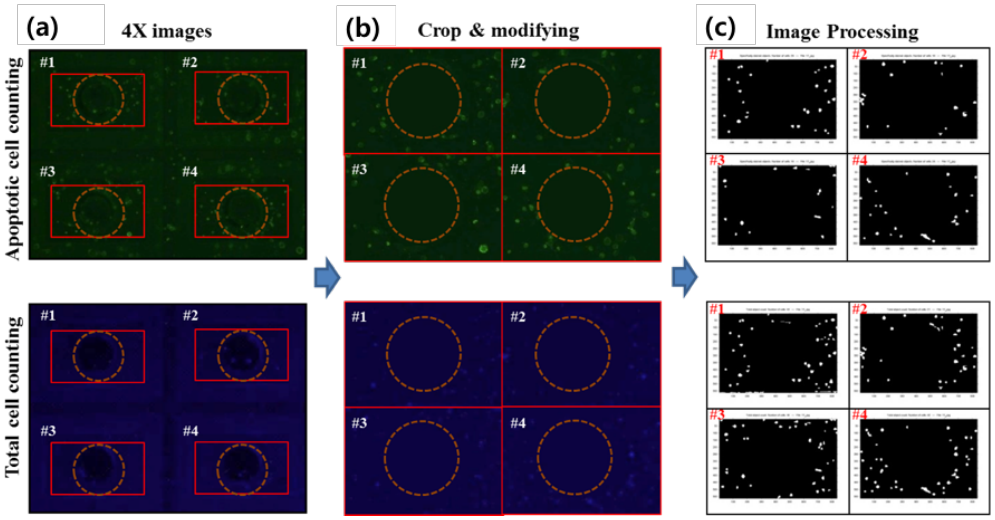

Figure 5.6 Image processing for apoptotic cell counting. (A) The 4X magnitude images are cropped to obtain regions of interest. Red rectangle represents region of interest and the orange circle represent the region of the microcapsule that need to be removed. (B) Each cropped image is further processed to remove background fluorescence noise came from the microcapsule. (C) The processed images were then analyzed by cell counting software to count the number of the apoptotic cells.

Chapter 6

Conclusion

In this dissertation, I have described new liquid-capped encoded microcapsules and their handling platform for the multiplex assays with the liquid microcapsule library. The encoded microcapsules-based liquid handling platform enables assays of large compound libraries in a single chip, eliminating the need for repeated dispensing steps and the aid of printing equipment or dispensing devices. By eliminating the equipment dependency for handling of the small volume liquid, and separating manufactures from users, this technique can easily provide individual researchers with a tool for performing the multiplex and high-throughput assays with decreased processing time, reagent costs and labor.

I developed a microfluidic platform that enables to encapsulate the nanoliter liquid inside the solid Teflon microcapsule. The chemically and biologically inert properties of the Teflon enable to encapsulate various liquid stably without evaporation and cross-contamination. Also, I developed a new encoding method which enables to identify liquid inside the microcapsule. By Utilizing

photoluminescence property of the photoinitiator after the UV exposure, I engraved the graphical code on the shell of the microcapsule for labeling of the liquid inside. This method offers much higher coding capacity than the conventional spectral coding scheme, without the need for any special coding material such as fluorescent dyes or quantum dots. Also, the graphical code enables to handle numerous kinds of liquids and to make a pooled chemical library by mixing and storing differently encoded microcapsules in a tube.

For the multiplex assay application with the encoded microcapsule, I developed a microwell array platform that enables to assemble thousands of heterogeneous encoded microcapsules in the microwell array by a single pipetting process. The graphical codes on the microcapsules enable to recognize liquid inside the microcapsules, even when they are randomly positioned in the microwells. Not only does the assembly process take just a few seconds, but it is also independent of the library size, a property that dramatically reduces the preparation time for heterogeneous dispensing of liquids. To release the liquid inside the microcapsule, I also developed a laser releasing system for selective releasing and a mechanical releasing system for high-throughput releasing. With the releasing system, various liquids inside the microcapsules can be released and reacted with the samples in the microwells, independently.

Finally, I compared the compatibility of our platform with a conventional platform by conducting an enzyme inhibitor screening, a virus transduction, and a drug-induced apoptosis testing. The results show that our platform can be used for various liquid-liquid reactions and liquid-cell reactions. Also, because of the reduced consumption of reagent, cells, and viruses, the platform can have a more impact especially when the amount of sample is insufficient for the conventional wellplate based experiments (e.g. rare cells or viruses). Although the UV sensitive materials such as RNAs or proteins are difficult to be encapsulated without damage, the simplicity and flexibility of our platform will promote the development of a range of bioassays, where the compounds are not UV sensitive, including cell-based assay, inhibitor screening, combinatorial drug screening, and other future applications.

Bibliography

[1] T. Thorsen, R. W. Roberts, F. H. Arnold, and S. R. Quake, "Dynamic Pattern Formation in a Vesicle-Generating Microfluidic Device," *Physical Review Letters,* vol. 86, pp. 4163-4166, 04/30/ 2001.

[2] Allon M. Klein, L. Mazutis, I. Akartuna, N. Tallapragada, A. Veres, V. Li, *et al.*, "Droplet Barcoding for Single-Cell Transcriptomics Applied to Embryonic Stem Cells," *Cell,* vol. 161, pp. 1187-1201.

[3] E. Brouzes, M. Medkova, N. Savenelli, D. Marran, M. Twardowski, J. B. Hutchison, *et al.*, "Droplet microfluidic technology for single-cell high-throughput screening," *Proceedings of the National Academy of Sciences,* vol. 106, pp. 14195-14200, August 25, 2009 2009.

[4] M. T. Guo, A. Rotem, J. A. Heyman, and D. A. Weitz, "Droplet microfluidics for high-throughput biological assays," *Lab on a Chip,* 2012.

[5] L.-F. Cai, Y. Zhu, G.-S. Du, and Q. Fang, "Droplet-Based Microfluidic Flow Injection System with Large-Scale Concentration Gradient by a Single Nanoliter-Scale Injection for Enzyme Inhibition Assay," *Analytical Chemistry,* vol. 84, pp. 446-452, 2012/01/03 2011.

[6] J.-C. Baret, O. J. Miller, V. Taly, M. Ryckelynck, A. El-Harrak, L. Frenz, *et al.*, "Fluorescence-activated droplet sorting (FADS): efficient microfluidic cell sorting based on enzymatic activity," *Lab on a Chip,* vol. 9, pp. 1850-1858, 2009.

[7] O. J. Miller, A. E. Harrak, T. Mangeat, J.-C. Baret, L. Frenz,

B. E. Debs, *et al.*, "High-resolution dose-response screening using droplet-based microfluidics," *Proceedings of the National Academy of Sciences,* vol. 109, pp. 378-383, January 10, 2012 2012.

[8] D. Hess, A. Rane, A. J. deMello, and S. Stavrakis, "High-Throughput, Quantitative Enzyme Kinetic Analysis in Microdroplets Using Stroboscopic Epifluorescence Imaging," *Analytical Chemistry,* vol. 87, pp. 4965-4972, 2015/05/05 2015.

[9] Evan Z. Macosko, A. Basu, R. Satija, J. Nemesh, K. Shekhar, M. Goldman, *et al.*, "Highly Parallel Genome-wide Expression Profiling of Individual Cells Using Nanoliter Droplets," *Cell,* vol. 161, pp. 1202-1214, 5/21/ 2015.

[10] E. X. Ng, M. A. Miller, T. Jing, D. A. Lauffenburger, and C.-H. Chen, "Low-volume multiplexed proteolytic activity assay and inhibitor analysis through a pico-injector array," *Lab on a Chip,* vol. 15, pp. 1153-1159, 2015.

[11] X. Niu, F. Gielen, J. B. Edel, and A. J. deMello, "A microdroplet dilutor for high-throughput screening," *Nat Chem,* vol. 3, pp. 437-442, 2011.

[12] R. Tewhey, J. B. Warner, M. Nakano, B. Libby, M. Medkova, P. H. David, *et al.*, "Microdroplet-based PCR enrichment for large-scale targeted sequencing," *Nat Biotech,* vol. 27, pp. 1025-1031, 11//print 2009.

[13] A. Huebner, S. Sharma, M. Srisa-Art, F. Hollfelder, J. B. Edel, and A. J. deMello, "Microdroplets: A sea of applications?," *Lab on a Chip,* vol. 8, pp. 1244-1254, 2008.

[14] A. B. Theberge, E. Mayot, A. El Harrak, F. Kleinschmidt, W. T. S. Huck, and A. D. Griffiths, "Microfluidic platform for combinatorial synthesis in picolitre droplets," *Lab on a Chip,* vol. 12, pp. 1320-1326, 2012.

[15] M. Muluneh, B. Kim, G. Buchsbaum, and D. Issadore, "Miniaturized, multiplexed readout of droplet-based microfluidic assays using time-domain modulation," *Lab on a Chip,* vol. 14, pp. 4638-4646, 2014.
[16] F. Shen, W. Du, E. K. Davydova, M. A. Karymov, J. Pandey, and R. F. Ismagilov, "Nanoliter Multiplex PCR Arrays on a SlipChip," *Analytical Chemistry,* vol. 82, pp. 4606-4612, 2010/06/01 2010.
[17] H. Song, D. L. Chen, and R. F. Ismagilov, "Reactions in Droplets in Microfluidic Channels," *Angewandte Chemie International Edition,* vol. 45, pp. 7336-7356, 2006.
[18] L. Mazutis, J. Gilbert, W. L. Ung, D. A. Weitz, A. D. Griffiths, and J. A. Heyman, "Single-cell analysis and sorting using droplet-based microfluidics," *Nat. Protocols,* vol. 8, pp. 870-891, 05//print 2013.
[19] J. J. Agresti, E. Antipov, A. R. Abate, K. Ahn, A. C. Rowat, J.-C. Baret*, et al.*, "Ultrahigh-throughput screening in drop-based microfluidics for directed evolution," *Proceedings of the National Academy of Sciences,* February 8, 2010 2010.
[20] H. Gu, M. H. G. Duits, and F. Mugele, "Droplets Formation and Merging in Two-Phase Flow Microfluidics," *International Journal of Molecular Sciences,* vol. 12, pp. 2572-2597, 04/15
02/17/received
03/11/revised
04/02/accepted 2011.
[21] E. Y. Basova and F. Foret, "Droplet microfluidics in (bio)chemical analysis," *Analyst,* vol. 140, pp. 22-38, 2015.
[22] S. Mashaghi, A. Abbaspourrad, D. A. Weitz, and A. M. van Oijen, "Droplet microfluidics: A tool for biology, chemistry and nanotechnology," *TrAC Trends in Analytical Chemistry,*

vol. 82, pp. 118-125, 9// 2016.
[23] D. J. Collins, A. Neild, A. deMello, A.-Q. Liu, and Y. Ai, "The Poisson distribution and beyond: methods for microfluidic droplet production and single cell encapsulation," *Lab on a Chip,* vol. 15, pp. 3439-3459, 2015.
[24] P. Zhu and L. Wang, "Passive and active droplet generation with microfluidics: a review," *Lab on a Chip,* vol. 17, pp. 34-75, 2017.
[25] T. S. Kaminski, S. Jakiela, M. A. Czekalska, W. Postek, and P. Garstecki, "Automated generation of libraries of nL droplets," *Lab on a Chip,* vol. 12, pp. 3995-4002, 2012.
[26] M. T. Guo, A. Rotem, J. A. Heyman, and D. A. Weitz, "Droplet microfluidics for high-throughput biological assays," *Lab on a Chip,* vol. 12, pp. 2146-2155, 2012.
[27] S. Fournier-Bidoz, T. L. Jennings, J. M. Klostranec, W. Fung, A. Rhee, D. Li*, et al.*, "Facile and Rapid One-Step Mass Preparation of Quantum-Dot Barcodes," *Angewandte Chemie International Edition,* vol. 47, pp. 5577-5581, 2008.
[28] P. P. T. Surawski, B. J. Battersby, G. A. Lawrie, K. Ford, A. Ruhmann, L. Marcon*, et al.*, "Flow cytometric detection of proteolysis in peptide libraries synthesised on optically encoded supports," *Molecular BioSystems,* vol. 4, pp. 774-778, 2008.
[29] V. Trivedi, A. Doshi, G. K. Kurup, E. Ereifej, P. J. Vandevord, and A. S. Basu, "A modular approach for the generation, storage, mixing, and detection of droplet libraries for high throughput screening," *Lab on a Chip,* vol. 10, pp. 2433-2442, 2010.
[30] X.-H. Ji, W. Cheng, F. Guo, W. Liu, S.-S. Guo, Z.-K. He*, et al.*, "On-demand preparation of quantum dot-encoded microparticles using a droplet microfluidic system," *Lab on a*

Chip, vol. 11, pp. 2561-2568, 2011.

[31] H. Q. Nguyen, B. C. Baxter, K. Brower, C. A. Diaz-Botia, J. L. DeRisi, P. M. Fordyce*, et al.*, "Programmable Microfluidic Synthesis of Over One Thousand Uniquely Identifiable Spectral Codes," *Advanced Optical Materials,* vol. 5, pp. 1600548-n/a, 2017.

[32] R. E. Gerver, R. Gomez-Sjoberg, B. C. Baxter, K. S. Thorn, P. M. Fordyce, C. A. Diaz-Botia*, et al.*, "Programmable microfluidic synthesis of spectrally encoded microspheres," *Lab on a Chip,* vol. 12, pp. 4716-4723, 2012.

[33] X. Gao and S. Nie, "Quantum Dot-Encoded Mesoporous Beads with High Brightness and Uniformity: Rapid Readout Using Flow Cytometry," *Analytical Chemistry,* vol. 76, pp. 2406-2410, 2004/04/01 2004.

[34] M. Han, X. Gao, J. Z. Su, and S. Nie, "Quantum-dot-tagged microbeads for multiplexed optical coding of biomolecules," *Nat Biotech,* vol. 19, pp. 631-635, 07//print 2001.

[35] G. A. Lawrie, B. J. Battersby, and M. Trau, "Synthesis of Optically Complex Core–Shell Colloidal Suspensions: Pathways to Multiplexed Biological Screening," *Advanced Functional Materials,* vol. 13, pp. 887-896, 2003.

[36] S. W. Birtwell and H. Morgan, "Microparticle Encoding Technologies for High-Throughput Multiplexed Suspension Assays

The Third International Conference on the Development of Biomedical Engineering in Vietnam." vol. 27, V. Toi and T. Q. D. Khoa, Eds., ed: Springer Berlin Heidelberg, 2010, pp. 316-319.

[37] L. Li, W. Du, and R. Ismagilov, "User-Loaded SlipChip for Equipment-Free Multiplexed Nanoliter-Scale Experiments," *Journal of the American Chemical Society,* vol. 132, pp. 106-

111, 2010/01/13 2009.

[38] J. Shemesh, T. Ben Arye, J. Avesar, J. H. Kang, A. Fine, M. Super*, et al.*, "Stationary nanoliter droplet array with a substrate of choice for single adherent/nonadherent cell incubation and analysis," *Proceedings of the National Academy of Sciences,* vol. 111, pp. 11293-11298, August 5, 2014 2014.

[39] W. Du, L. Li, K. P. Nichols, and R. F. Ismagilov, "SlipChip," *Lab on a Chip,* vol. 9, pp. 2286-2292, 2009.

[40] Y. Zhu, Y.-X. Zhang, L.-F. Cai, and Q. Fang, "Sequential Operation Droplet Array: An Automated Microfluidic Platform for Picoliter-Scale Liquid Handling, Analysis, and Screening," *Analytical Chemistry,* vol. 85, pp. 6723-6731, 2013/07/16 2013.

[41] Y. Zhang, Y. Zhu, B. Yao, and Q. Fang, "Nanolitre droplet array for real time reverse transcription polymerase chain reaction," *Lab on a Chip,* vol. 11, pp. 1545-1549, 2011.

[42] F. Shen, B. Sun, J. E. Kreutz, E. K. Davydova, W. Du, P. L. Reddy*, et al.*, "Multiplexed Quantification of Nucleic Acids with Large Dynamic Range Using Multivolume Digital RT-PCR on a Rotational SlipChip Tested with HIV and Hepatitis C Viral Load," *Journal of the American Chemical Society,* vol. 133, pp. 17705-17712, 2011/11/09 2011.

[43] R. R. Pompano, W. Liu, W. Du, and R. F. Ismagilov, "Microfluidics Using Spatially Defined Arrays of Droplets in One, Two, and Three Dimensions," *Annual Review of Analytical Chemistry,* vol. 4, pp. 59-81, 2011.

[44] H. Li, S. Bergeron, and D. Juncker, "Microarray-to-Microarray Transfer of Reagents by Snapping of Two Chips for Cross-Reactivity-Free Multiplex Immunoassays," *Analytical Chemistry,* vol. 84, pp. 4776-4783, 2012/06/05

2012.
[45] A. A. Popova, K. Demir, T. G. Hartanto, E. Schmitt, and P. A. Levkin, "Droplet-microarray on superhydrophobic-superhydrophilic patterns for high-throughput live cell screenings," *RSC Advances,* vol. 6, pp. 38263-38276, 2016.
[46] A. A. Popova, S. M. Schillo, K. Demir, E. Ueda, A. Nesterov-Mueller, and P. A. Levkin, "Droplet-Array (DA) Sandwich Chip: A Versatile Platform for High-Throughput Cell Screening Based on Superhydrophobic-Superhydrophilic Micropatterning," *Advanced Materials,* vol. 27, pp. 5217-5222, 2015.
[47] G.-S. Du, J.-Z. Pan, S.-P. Zhao, Y. Zhu, J. M. J. den Toonder, and Q. Fang, "Cell-Based Drug Combination Screening with a Microfluidic Droplet Array System," *Analytical Chemistry,* vol. 85, pp. 6740-6747, 2013/07/16 2013.
[48] W.-B. Du, M. Sun, S.-Q. Gu, Y. Zhu, and Q. Fang, "Automated Microfluidic Screening Assay Platform Based on DropLab," *Analytical Chemistry,* vol. 82, pp. 9941-9947, 2010/12/01 2010.
[49] S. Zeng, B. Li, X. o. Su, J. Qin, and B. Lin, "Microvalve-actuated precise control of individual droplets in microfluidic devices," *Lab on a Chip,* vol. 9, pp. 1340-1343, 2009.
[50] J. P. Rolland, R. M. Van Dam, D. A. Schorzman, S. R. Quake, and J. M. DeSimone, "Solvent-Resistant Photocurable "Liquid Teflon" for Microfluidic Device Fabrication," *Journal of the American Chemical Society,* vol. 126, pp. 2322-2323, 2004/03/01 2004.
[51] Y. Huang, P. Castrataro, C.-C. Lee, and S. R. Quake, "Solvent resistant microfluidic DNA synthesizer," *Lab on a Chip,* vol. 7, pp. 24-26, 2007.

[52] N. S. G. K. Devaraju and M. A. Unger, "Multilayer soft lithography of perfluoropolyether based elastomer for microfluidic device fabrication," *Lab on a Chip,* vol. 11, pp. 1962-1967, 2011.

[53] R. Bongiovanni, A. Medici, A. Zompatori, S. Garavaglia, and C. Tonelli, "Perfluoropolyether polymers by UV curing: design, synthesis and characterization," *Polymer International,* vol. 61, pp. 65-73, 2012.

[54] A. Vitale, M. Quaglio, M. Cocuzza, C. F. Pirri, and R. Bongiovanni, "Photopolymerization of a perfluoropolyether oligomer and photolithographic processes for the fabrication of microfluidic devices," *European Polymer Journal,* vol. 48, pp. 1118-1126, 2012.

[55] M. A. Zieringer, N. J. Carroll, A. Abbaspourrad, S. A. Koehler, and D. A. Weitz, "Microcapsules for Enhanced Cargo Retention and Diversity," *Small,* vol. 11, pp. 2903-2909, 2015.

[56] C. Kim, S. Chung, Y. E. Kim, K. S. Lee, S. H. Lee, K. W. Oh, *et al.*, "Generation of core-shell microcapsules with three-dimensional focusing device for efficient formation of cell spheroid," *Lab on a Chip,* vol. 11, pp. 246-252, 2011.

[57] S. S. Datta, S.-H. Kim, J. Paulose, A. Abbaspourrad, D. R. Nelson, and D. A. Weitz, "Delayed Buckling and Guided Folding of Inhomogeneous Capsules," *Physical Review Letters,* vol. 109, p. 134302, 2012.

[58] S. S. Datta, A. Abbaspourrad, E. Amstad, J. Fan, S.-H. Kim, M. Romanowsky, *et al.*, "25th Anniversary Article: Double Emulsion Templated Solid Microcapsules: Mechanics And Controlled Release," *Advanced Materials,* vol. 26, pp. 2205-2218, 2014.

[59] S. J. Pastine, D. Okawa, A. Zettl, and J. M. J. Fréchet, "Chemicals On Demand with Phototriggerable

Microcapsules," *Journal of the American Chemical Society,* vol. 131, pp. 13586-13587, 2009.

[60] P. W. Chen, R. M. Erb, and A. R. Studart, "Designer Polymer-Based Microcapsules Made Using Microfluidics," *Langmuir,* vol. 28, pp. 144-152, 2012/01/10 2011.

[61] S.-H. Kim, J. W. Kim, J.-C. Cho, and D. A. Weitz, "Double-emulsion drops with ultra-thin shells for capsule templates," *Lab on a Chip,* vol. 11, pp. 3162-3166, 2011.

[62] H. N. Yow and A. F. Routh, "Formation of liquid core-polymer shell microcapsules," *Soft Matter,* vol. 2, pp. 940-949, 2006.

[63] B. Wu, H.-Q. Gong, and R. Zhang, "Maskless formation of chromatic-pattern barcodes in two-component microcapsules," *Microfluidics and Nanofluidics,* pp. 1-6, 2013/10/25 2013.

[64] M. A. Zieringer, N. J. Carroll, A. Abbaspourrad, S. A. Koehler, and D. A. Weitz, "Microcapsules for Enhanced Cargo Retention and Diversity," *Small,* pp. n/a-n/a, 2015.

[65] S.-H. Kim, J.-G. Park, T. M. Choi, V. N. Manoharan, and D. A. Weitz, "Osmotic-pressure-controlled concentration of colloidal particles in thin-shelled capsules," *Nat Commun,* vol. 5, 2014.

[66] A. Abbaspourrad, N. J. Carroll, S.-H. Kim, and D. A. Weitz, "Polymer Microcapsules with Programmable Active Release," *Journal of the American Chemical Society,* vol. 135, pp. 7744-7750, 2013/05/22 2013.

[67] S. Seiffert, J. Thiele, A. R. Abate, and D. A. Weitz, "Smart Microgel Capsules from Macromolecular Precursors," *Journal of the American Chemical Society,* vol. 132, pp. 6606-6609, 2010/05/12 2010.

[68] Y. Hennequin, N. Pannacci, C. P. de Torres, G. Tetradis-Meris, S. Chapuliot, E. Bouchaud*, et al.*, "Synthesizing

Microcapsules with Controlled Geometrical and Mechanical Properties with Microfluidic Double Emulsion Technology," *Langmuir,* vol. 25, pp. 7857-7861, 2009/07/21 2009.

[69] J. S. Jyrki Selinummi, Olli Yli-Harja, Jaakko A. Puhakka, "Software for quantification of labeled bacteria from digital microscope images by automated image analysis," *BioTechniques,* vol. 39, pp. 859-863, 2005.

국문 초록

대부분의 생명공학, 화학 관련 실험에서는 반응 시간 및 시약의 비용을 줄이기 위해 적은 부피의 액체를 다루는 것을 선호하고 이를 위해서 마이크로피펫을 이용하는 것이 보편적이다. 기존의 마이크로피펫의 경우 수백 마이크로리터에서 수 마이크로리터 정도 부피의 액체를 다룰 수 있는데, 이보다 더 적은 부피, 예를 들어 나노 리터의 액체를 다루는 경우 기존의 마이크로피펫의 경우 불가능하다. 이런 이유로, 적은 부피의 액체를 다룰 수 있는 여러 기술들 또한 개발되고 있는 상황이다.

여러 기술들 중, 미세유체기술을 이용한 드랍렛 (droplet) 기술은 물과 기름과 같이 서로 섞이지 않는 액체를 이용, 수 나노 리터 부피의 액체 방울을 만들고 이를 증발하지 않게 보관, 다른 액체방울과의 반응을 유도할 수 있는 기술로 현재까지도 많은 연구소에서 연구를 진행중인 기술이다. 이 드랍렛 기술은 단일 시약을 매우 적은 부피로 분석할 필요가 있는 분야의 경우 매우 큰 장점이 있지만, 다중 분석 (multiplex assay) 과 같은 다양한 시약을 이용하여 분석하는 실험의 경우 그 사용이 제한되고 있는데, 가장 큰 이유로는 다양한 시약을 포함하고 있는 액체 방울 각각을 구별 할 수 있는 코드를 부여하기가 어렵기 때문이다.

본 논문에서는 수 나노 리터 부피의 액체 방울을 내부에 함유하고 있는 마이크로캡슐을 만들고 캡슐의 껍질에 그래픽 코드를 새기는 방법을 개발하여 코드화된 마이크로캡슐을 제작, 각각의 액체 방울을 구별 할 수 있도록 하였다. 이렇게 만들어진 코드화된 마이크로캡슐은 다중 분석을 위해 마이크로웰 어레이에 조립되는데, 한번의 피펫팅 작업을 통해 수많은 마이크로캡슐을 마이크로웰 어레이에 조립할 수 있는 기술 또한 개발하였고, 조립된 각각의 마이크로캡슐 내부의 액체를 외부로 방출하는 기술 또한 개발하였다. 또한 코드화된 마이크로캡슐이 실제 다중 분석에 적용 가능함을 보여주기 위해 효소 저해제 스크리닝 (enzyme-inhibitor screening), 바이러스 형질 도입 (virus transduction) 및 항암제를 이용한 세포독성 스크리닝 (drug-induced apoptosis assay) 등을 수행하였고, 코드화된 마이크로캡슐을 이용한 결과와 기존의 웰 플레이트를 통해 수행한 결과가 비슷함을 보였다. 이 기술을 이용하면 기존 분석 방법에 비해 수 백배 적은 양의 시약 또는 세포를 이용하여 실험을 수행할 수 있기 때문에 기존 웰 플레이트를 통해 수행하기에는 그 양이 충분하지 않은 희귀 세포(rare cell)나 바이러스를 이용한 실험의 경우 매우 유용한 기술이 될 거라 예상한다.

주요어 : 코드화된 마이크로캡슐, 액체 캡슐화, 미세액적 라벨링, 다중 분석

학번 : 2009-23116